Pax3- and Pax7-mediated Dbx1 regulation orchestrates the patterning of intermediate spinal interneurons

Chris Gard, Gloria Gonzalez Curto, Youcef El-Mokhtar, Elodie Chollet, Nathalie Duval, Valentine Auzié, Frédéric Auradé, Lisa Vigier, Frédéric Relaix, Alessandra Pierani, et al.

Pax3- and Pax7-mediated Dbx1 regulation orchestrates the patterning of intermediate spinal interneurons

Chris GARD[1*], Gloria GONZALEZ-CURTO[1*], Youcef El-Mokhtar FRARMA[1], Elodie CHOLLET[1], Nathalie DUVAL[1,2], Valentine AUZIÉ[1], Frédéric AURADÉ[3,4], Lisa VIGIER[1], Frédéric RELAIX[4], Alessandra PIERANI[1], Frédéric CAUSERET[1#] & Vanessa RIBES[1#]

[1] Institut Jacques Monod, CNRS UMR7592, Université Paris Diderot, Sorbonne Paris Cité, 75205 Paris Cedex, France

[2] Institut Pasteur, Department of developmental and stem cell biology, CNRS URA 2578, 75015 Paris, France

[3] Sorbonne Universités UPMC Univ Paris 06, Inserm, CNRS, Centre de Recherche en Myologie (CRM), GH Pitié Salpêtrière, 47 bld de l'hôpital, 75013 Paris, France

[4] INSERM IMRB U955-E10, UPEC - Université Paris Est, Faculté de Médicine, Créteil 94000, France

* these authors have equally contributed to the study

corresponding authors:

vanessa.ribes@ijm.fr

frederic.causeret@inserm.fr

Abstract

Transcription factors are key orchestrators of the emergence of neuronal diversity within the developing spinal cord. As such, the two paralogous proteins Pax3 and Pax7 regulate the specification of progenitor cells within the intermediate neural tube, by defining a neat segregation between those fated to form motor circuits and those involved in the integration of sensory inputs. To attain insights into the molecular means by which they control this process, we have performed detailed phenotypic analyses of the intermediate spinal interneurons (IN), namely the dI6, $V0_D$, $V0_{VCG}$ and V1 populations in compound null mutants for Pax3 and Pax7. This has revealed that the levels of Pax3/7 proteins determine both the dorso-ventral extent and the number of cells produced in each subpopulation; with increasing levels leading to the dorsalisation of their fate. Furthermore, thanks to the examination of mutants in which Pax3 transcriptional activity is skewed either towards repression or activation, we demonstrate that this cell diversification process is mainly dictated by Pax3/7 ability to repress gene expression. Consistently, we show that Pax3 and Pax7 inhibit the expression of *Dbx1* and of its repressor *Prdm12*, fate determinants of the V0 and V1 interneurons, respectively. Notably, we provide evidence for the activity of several *cis*-regulatory modules of *Dbx1* to be sensitive to Pax3 and Pax7 transcriptional activity levels. Altogether, our study provides insights into how the redundancy within a TF family, together with discrete dynamics of expression profiles of each member, are exploited to generate cellular diversity. Furthermore, our data supports the model whereby cell fate choices in the neural tube do not rely on binary decisions but rather on inhibition of multiple alternative fates.

Highlights

- Pax3 and Pax7 control the spatial organisation of spinal differentiation
- Pax3 and Pax7 repressive activity spatially restricts Dbx1 and Prdm12 expression
- An intronic *cis*-regulatory module recapitulates *Dbx1* expression
- The *Dbx1* intronic *cis*-regulatory module is sensitive to Pax3/7 transcriptional activity

Keywords

Neuronal patterning; Pax3/Pax7 transcription factors; Dbx1; repression; spinal cord interneurons; *cis*-regulatory modules.

Introduction

The developing vertebrate neural tube is a classical and well-studied model to address how cell diversity is generated and organised within a tissue. The stereotypical arrangements and numbers of neuronal subtypes composing the adult spinal cord emanate from two rounds of cell-fate choices operating during embryogenesis (Lai et al., 2016; Lu et al., 2015). During the first phase, "naïve" progenitor cells acquire distinct molecular signatures depending on their position along the dorsal-ventral (D-V) axis of the neural tube (Del Corral and Storey, 2004; Lai et al., 2016; Lu et al., 2015). These signatures are then further variegated when cells undergo post-mitotic differentiation. Ultimately, cells will express unique sets of genes imposing stereotypic physiological and morphological traits upon each neuronal subtype. This process of cellular determination is largely controlled by transcription factors (TFs) (Lai et al., 2016; Lu et al., 2015). These proteins operate at the level of non-coding *cis*-regulatory modules (CRMs) where they recruit factors impacting on the activity of the basal transcriptional machinery and/or the chromatin state. Thereby, their activity underpins the overall levels of gene activation or repression within cells (Spitz and Furlong, 2012). Although the extent of TF diversity within the developing vertebrate neural tube can now be estimated (e.g. Armant et al., 2013, see also Supp. Table 4), how their activity at the level of CRMs generates robust gene expression profiles and cellular phenotypes is still poorly defined and hence remains under intensive investigation (e.g. Bailey et al., 2006; Borromeo et al., 2014; Kutejova et al., 2016; Mazzoni et al., 2013).

To delve into this issue, we focussed on the activity of two paralogous and highly related proteins, Pax3 and Pax7 (Mayran et al., 2015). These TFs are amongst the first to be induced within the dorsal part of the developing spinal cord; in mouse, Pax3 is induced by gestational day (GD) 8, while Pax7 appears 24 hours later (Goulding et al., 1991; Jostes et al., 1990). It has

been known for a long time that these factors are essential to spinal cord development and control several key cellular processes ranging from neural tube closure to timing of post-mitotic differentiation (e.g. Epstein et al., 1991; Nakazaki et al., 2008). In addition, several studies have led to the idea that these factors orchestrate cell type specification not only within the dorsal neural tube where they are expressed (Moore et al., 2013; Nakazaki et al., 2008) but also within the intermediate neural tube (Mansouri and Gruss, 1998). In this region, 3 adjacent progenitor pools, dp6, p0 and p1 (from dorsal to ventral), are fated to become dI6, V0 and V1 interneurons (IN), respectively (Lu et al., 2015). The V1 and V0 IN populations are further diversified into discrete neuronal subtypes. For instance, the most dorsal p0 progenitors give rise to two GABA- and glycine-secreting populations, termed $V0_D$ and $V0_V$ IN, while the ventral p0 progenitors give rise to two excitatory neuronal subtypes, the cholinergic $V0_C$ and glutamatergic $V0_G$ IN (Lu et al., 2015). Within these populations, it was previously shown that the position and the number of V1 and $V0_{VCG}$ IN are regulated by Pax3 and Pax7 activity; in their absence, the V1 IN are produced in excess and are intermingled with V0 IN (Mansouri and Gruss, 1998). Whether Pax3 and Pax7 regulate the fate of the other intermediate cell types remains to be tested and the molecular mechanisms by which they repress ventral fates needs to be established. Notably, it is still unclear whether they are able to directly repress the expression of ventral specifiers. Indeed, even though both Pax3 and Pax7 possess an octapeptide motif capable of interactions with the Groucho/TLE co-repressors (Muhr et al., 2001), most studies suggest that they act as transcriptional activators. For instance, Pax3 and Pax7 have been shown to be necessary to promote the activity of CRMs regulating the expression of key patterning genes such as Pax3 itself or Neurog2 (Moore et al., 2013; Nakazaki et al., 2008). Further supporting this, the expression of a single functional allele of Pax3 encoding an activator form of Pax3 is sufficient to rescue many of the morphological defects of Pax3 single mutants (Relaix et al., 2003).

Altogether these data prompted us to assess the precise contribution of Pax3 and Pax7 to the patterning of the intermediate neural tube and to test whether their active and/or repressive transcriptional activity is involved in this process. To this end, we have analysed the distribution of intermediate interneuron populations in mouse embryos carrying either compound null mutations for these two genes or dominant active or repressive forms of Pax3. These analyses revealed that the modulation of the levels and the type of transcriptional activity determines not only the position but also the number of neurons generated. Furthermore, they led us to identify Prdm12 and Dbx1 as target genes, the latter being capable of sensing the levels of Pax3 and Pax7 transcriptional activity through several *cis*-regulatory modules.

Material and Methods

Mouse lines and *in ovo* electroporation

Mice carrying *Pax3* null, *PAX3A*, *Pax3R* and *Pax7* null alleles were previously described (Bajard et al., 2006; Mansouri et al., 1996; Relaix et al., 2005, 2003). Notably, *PAX3A* and *Pax3R* alleles encode for proteins made of Pax3 DNA-binding domains fused to either the FOXO1 transactivation or Engrailed repressor domain. These are expressed from the *Pax3* locus upon activation of the Cre recombinase driven by the zygote specific *PGK* enhancer (Lallemand et al., 1998). Electroporation constructs expressing Pax3 and Pax7 variants and Dbx1 from the *pCIG* vector engineered to bi-cistronically express nuclear-targeted GFP (Megason and McMahon, 2002) were generated. The *CRM4.8kb*, which contains the *Dbx1* minimal promoter and the *CRM4.8kb::iCRM* were cloned into a *pBluescript* vector, while *CRM1* to *3* and the *iCRM* were inserted into a *bGZA* vector (Yee et al., 1993), upstream of a minimal *HBB* promoter. For detailed cloning strategies see Supp. Material and Methods. Reporter plasmids (0.5µg/µl) and *pCIG* based constructs (1.5 µg/µl) were electroporated in

Hamburger and Hamilton (HH) stage 10-11 chick embryos according to described protocols (Briscoe et al., 2000).

Immunohistochemistry and *in situ* hybridisation

Mouse and chick embryos were fixed in 4% paraformaldehyde for 45 min to 2 hr at 4°C. Fixed embryos were cryoprotected by equilibration in 15% sucrose, embedded in gelatin, cryosectioned (14 μm), and processed for immunostaining (Briscoe et al., 2000) or *in situ* hybridisation (ISH) (Yamada et al., 1993). Details of the reagents are provided in the Supp. Material and Methods. All quantifications were performed at brachial levels using ImageJ v.1.43 g image analysis software (NIH) on usually more than 3 embryos and on 2 to 4 transverse sections per embryo (Supp. Table 1, Table 2). The number of cells per section was determined using the cell counter plugin. Fluorescence intensity of β-Galactosidase and of GFP in chick embryos and the evaluation of dorsal–ventral boundaries position were determined as described in (Balaskas et al., 2012). The heat maps were generated using MATLAB (Mathworks, Natick, MA) and correspond to the mean of the ratios of β-Galactosidase fluorescence intensity over that of GFP on the number of sections and embryos indicated in Supp. Table 2. The heat maps provide a color-coded scale for individual datasets by associating the lowest value in the data matrix with dark blue and the highest value with dark red. All statistical analyses were performed using a Mann-Whitney U test in GraphPad Prism and all the p-values are given in Supp. Table 3.

In silico analysis of *Dbx1* locus

The mouse sequence of each CRM was used as the query sequence for cross-species BLAT searches, performed with the Ensembl genome browser (http://www.ensembl.org/). The alignments of enhancer sequences across anole lizard, cat, chicken, chimpanzee, Chinese soft-

shell turtle, cow, horse, human, mouse, rat, xenopus and zebrafish genomes were produced and analysed using ClustalOmega (http://www.ebi.ac.uk/Tools/msa/clustalo/) and phylogenetically conserved motifs were defined using MEME (http://meme.ebi.edu.au/meme/tools/meme). Putative TF binding sites within the conserved motifs were identified using the Tomtom tool in the MEME suite (http://meme.ebi.edu.au/meme/tools/tomtom). The alignments of enhancer sequences were searched for putative Pax3 and Pax7 homeodomain and paired binding sites using position weight matrices (PWMs) for these sites using FIMO (http://meme-suite.org/tools/fimo). PWMs for Pax homeodomain binding sites were either taken from work by (Jolma et al., 2013) or created *de novo* from Pax3 and Pax7 ChIP-Sequencing data (Soleimani et al., 2012) using MEME (Supp. Fig. 3A, Supp. Material and Methods). To characterise the functionality of Dbx1 CRMs, H3K27ac, H3K4me1, DNase-seq and enhancer-like predictions from mouse GD11.5 and/or GD12.5 neural tube reference epigenome data were obtained from the ENCODE data center (Encode project consortium, 2012). Data were produced by the B. Ren (UCSD) and Z. Weng (Umass) laboratories and can be retrieved under the ENCODE project accession numbers ENCSR111SYT, ENCSR362MIE, ENCSR003PNR, ENCSR448TTC and ENCSR263CKR. Sox2 and Sox3 binding events in neural progenitors were obtained from Bergsland et al. (2012). Pax7 binding events in muscle were obtained from Soleimani et al. (2012). Processed data in mm9 assembly coordinates were transformed into mm10 using the UCSC LiftOver tool.

RESULTS

Modulations in the levels of Pax3 and Pax7 transcriptional activities impact on the specification of intermediate spinal interneurons

In order to analyse the fate of intermediate dp6 to p1 progenitors upon the modulation of Pax3 and Pax7 transcriptional activity, we analysed the expression profiles of several TFs allowing

the identification of dI6, $V0_D$, $V0_{VCG}$ and V1 IN in several mutants for Pax3 and Pax7 (Fig. 1)(Lai et al., 2016; Lu et al., 2015). To distinguish dI6 IN we performed immunolabelling for Lbx1 together with AP2α and/or Brn3a; the dI6 express only Lbx1, while the abutting dorsal dI5 population is $Lbx1^+$, $AP2\alpha^+$, $Brn3a^+$ (Supp. Fig. 1A-D, Fig. 1Ai, C). Detecting Pax2 and Lbx1 allowed us to identify $V0_D$ IN, as a $Pax2^+/Lbx1^-$ population ventrally flanking $Pax2^+/Lbx1^+$ dI6 cells (Fig. 1Aviii, C). The identification of this $V0_D$ population can be facilitated by the additional labelling of Evx1, allowing to distinguish between $Evx1^-$ $V0_D$ and $Evx1^+$ $V0_{VCG}$ IN populations (Fig. 1Aviii). Finally, V1 IN were observed by visualising FoxD3 expression (Fig. 1Axv, C).

These immunolabellings revealed that the generation of dI6 IN is not dramatically affected by the loss of either Pax3 or Pax7 (Fig. 1Ai, ii, Bi and data not shown). However, their number greatly decreases in $Pax3^{-/-}$;$Pax7^{+/-}$ embryos and even more in double knock-out (dKO) embryos (Fig. 1Aiii, iv, Bi). This indicates that production of dI6 IN requires both Pax3 and Pax7 activities and is sensitive to gene dosage. Similar conclusions can be drawn for the $V0_D$ IN. The decrease in their number seen in $Pax3^{-/-}$ single mutants is accentuated by the loss of one allele of Pax7 (Fig. 1Aviii-x, Bii). The dKO embryos display barely any $V0_D$ cells (Fig. 1Axi, Supp. Fig. 1E). However, precise quantification was compromised by the GFP expressed from Pax3 mutant alleles and the absence of the $Pax2^-$ $V0_V$ population that normally separates the $Pax2^+$ $V0_D$ from the $V0_{CG}$/V1 cells (Fig. 1Axi, Fig. 1C, (Lai et al., 2016; Lu et al., 2015)). In contrast with dI6 and $V0_D$ IN, the number of $Evx1^+$ $V0_{VCG}$ IN is increased in Pax3 single null mutants (Fig. 1Axv, xvi, Biii). This expansion is further increased in absence of one allele of Pax7, indicating that the generation of this population is restricted by Pax3 and Pax7 and that the restriction is dependent on Pax3/7 levels (Fig. 1Axvii, Biii). Intriguingly, the $V0_{VCG}$ population is very much reduced in dKO embryos (Fig. 1Axviii, Biii). This can be correlated with the dramatic dorsal expansion of $FoxD3^+$ V1 cells observed in absence of both Pax3 and Pax7 (Fig.

1Axv, xviii, Biv), which was also previously observed using *in situ* hybridisation labelling of *EN1* mRNA, a V1 determinant (Mansouri and Gruss, 1998). This dorsal expansion of V1 IN was also observed, although to a lesser extent, in $Pax3^{-/-};Pax7^{+/-}$ embryos and is even less pronounced in $Pax3^{-/-}$ embryos (Fig. 1Axvi, xvii, Biv). Taken together these analyses demonstrate that the number and the position of dI6, $V0_D$, $V0_{VCG}$ and V1 IN are regulated by the levels of Pax3 and Pax7 proteins, with dorsal fates being progressively converted to ventral ones upon loss of Pax3/7 alleles.

To assess whether Pax3/Pax7-mediated patterning of the intermediate spinal cord involves transcriptional activation or repression, we performed the same immunostainings on brachial sections of embryos expressing a dominant active (PAX3A) or repressive form (Pax3R) of Pax3 from the Pax3 locus (Fig. 1). Upon PAX3A expression, the generation of dI6 IN is completely lost, while the expression of Pax3R has little, if any, effect on this population (Fig. 1Av-vii, Bv). Taken together with the progressive loss of dI6 IN when Pax3/Pax7 alleles are successively removed, this indicates that the generation of dI6 IN requires Pax3/7 repressive activity. Conversely, the $V0_D$ population, which is also decreased upon loss of Pax3/7 alleles, expands upon the expression of PAX3A and recedes slightly upon expression of Pax3R (Fig. 1Axii-xiv, Bvi), suggesting that the fate of this population is more dependent on Pax3 positive activity. $V0_{VCG}$ IN are also affected by the expression of the transcriptional active and repressive forms of Pax3. Expression of PAX3A increases the population, while it is reduced in $Pax3^{KIPax3R/-}$ embryos (Fig. 1Axix-xxi, Bvii), suggesting that Pax3 repressive activity prevents $V0_{VCG}$ IN generation. Finally and intriguingly, contrasting with the dKO phenotype, the V1 population is neither affected by the expression of PAX3A nor by that of Pax3R. Several hypotheses can be drawn to explain this phenotype. First, the ventral restrictions of the V1 population by Pax3 and Pax7 depend on a complex regulatory network, implicating both their positive and negative

transcriptional potential. Second, the remaining two alleles of Pax7 in embryos carrying the Pax3R and PAX3A alleles may interfere, thus rendering the interpretation of these results difficult. To conclude, our data demonstrate that the levels of Pax3 and Pax7 activity, notably those leading to transcriptional repression, play a key role in the positioning and numbering of four distinct interneuron populations of the intermediate neural tube.

Pax3 and Pax7 repressive transcriptional activity restricts the Dbx1 dorsal boundary

Amongst the known TFs that regulate the fate of neurons within the intermediate spinal cord and that could be targeted by Pax3 and Pax7, Dbx1 stood out. Dbx1 is mainly expressed by p0 progenitors in a domain that just overlaps with that of Pax7 ((Dessaud et al., 2010; Dyck et al., 2012; Lanuza et al., 2004; Pierani et al., 2001) and is able to direct spinal progenitor cells towards a V0 fate by preventing them from adopting either a V1 or a dI6 fate ((Lanuza et al., 2004; Pierani et al., 2001), Fig. 4A, Supp. Fig. 1F). To evaluate the possibility of Pax3/7 regulating Dbx1, we first compared the dynamics in the expression profile of these three TFs in mouse embryos in which the stable reporter proteins GFP and β–Galactosidase are expressed from *Pax3* and *Pax7* loci, respectively (Fig. 2A, Supp. Fig. 2A, data not shown). Pax7 is induced in the neural tube concomitantly with Dbx1 around GD9.0 (data not shown; (Jostes et al., 1990; Pierani et al., 1999)) and at all stages analysed their expression only overlaps within the most dorsal row of the $Dbx1^+$ domain (Fig. 2Aii', Supp. Fig. 2A). Within this row of cells, Pax3 is also detected (Fig. 2Aii), with $Pax3^+$ cells representing less than 20% of $Dbx1^+$ cells (Fig. 2Aiii). This contrasts with the presence of Pax3 lineage marker GFP in more than 98% of $Dbx1^+$ cells (Fig. 2Aiii). Dbx1 induction, thus, appears temporally correlated with the dynamic dorsal restriction of Pax3 expression (Fig. 2B). Dbx1 induction may then be stabilised by a Dbx1

mediated repression of Pax3, as illustrated by the downregulation of Pax3 and, to a lesser extent of Pax7, upon Dbx1 gain of function in chick embryos (Fig. 4Aii, iii).

We then assessed whether *Dbx1* expression is modulated by the loss of function of Pax3 and Pax7 by performing *in situ* hybridisation against *Dbx1* transcripts in *Pax3* and *Pax7* double null mutant mice at GD10.5 and GD11.5 (Fig. 2C, Supp. Fig. 2B). At both stages, the *Dbx1*$^{+}$ domain is dorsally expanded within the neural tube of double mutants and reaches a size double that of control embryos. To further determine the contribution of Pax3 and/or Pax7 to *Dbx1* ventral restriction, we examined Dbx1 protein distribution in several compound null mutants for both genes at GD11.5 (Fig. 2D, Supp. Fig. 2C, Di). In *Pax7* null mutants, the Dbx1 expression profile remains unchanged (Supp. Fig. 2C). Conversely, a slight, yet significant, increase in the number of Dbx1^{+} cells was observed in *Pax3* single mutants (Fig. 2Di, ii, v). This phenotype appears stronger upon removal of one *Pax7* allele (Fig. 2Diii, v). Indeed, in *Pax3*$^{-/-}$*; Pax7*$^{+/-}$ embryos, not only is the Dbx1^{+} domain dorsally expanded (Supp. Fig. 2Di), but also all of the cells within this domain express Dbx1 protein. By contrast, in control embryos, Dbx1 protein distribution is present in a salt-and-pepper pattern (compare Fig. 2Diii to Fig. 2Di). Intriguingly, despite the large expansion of *Dbx1* transcript distribution in *Pax3;Pax7* double mutants (Supp. Fig. 2Di), we observed a reduced number of cells expressing Dbx1 protein compared to control embryos (Fig. 2Div, v); suggesting post-transcriptional down-regulation of Dbx1 in the absence of Pax3 and Pax7. This could explain the reduction of V0$_{VCG}$ IN production previously observed in dKO mutants (Fig. 1Axviii, Biii). Taken together these results indicate that both Pax3 and Pax7 are required to position the dorsal border of the *Dbx1* expression domain.

We then sought to evaluate whether gain of function for Pax3 and Pax7 impacts on *Dbx1* expression. For this, we electroporated chick embryos at Hamilton and Hamburger stage HH10-11 with constructs driving the bi-cistronic expression of either Pax3 or Pax7 together with GFP (Fig. 2E). At 24 hours post electroporation (hpe), both Pax3 and Pax7 ectopic expression are

sufficient to prevent the induction of *Dbx1* transcription, while electroporation of the empty *GFP* containing plasmid (*pCIG*) has no effect.

Altogether, these results prompted us to investigate whether Pax3- and Pax7-mediated restriction of *Dbx1* expression occurs by transcriptional activation or repression (Drouin, 2014). First, we analysed the distribution of *Dbx1* mRNA and protein in mouse embryos expressing Pax3R or PAX3A, at GD10.5 and GD11.5. (Fig. 2F-H, Supp. Fig. 2Dii). Embryos carrying the *Pax3R* allele display a reduction in the levels of Dbx1 transcripts and protein (Fig. 2F, G). Upon quantification, no significant changes in the position of Dbx1 D-V boundaries were noted in mutants carrying a *Pax3R* allele compared to control embryos (Fig. 2Fv, Supp. Fig. 2Dii). By contrast, in $Pax3^{Pax3A/+}$ embryos, the Dbx1 domain is more than doubled in size at GD10.5 (Fig. 2Fiv, v, 2Giv, v) and further expands with time to encompass the entire dorsal region of the spinal cord in GD11.5 embryos (Fig. 2Hi, ii). In addition, this expansion occurs both dorsally and ventrally, unlike the purely dorsal expansion observed in double knockout embryos (Fig. 2Fv, Supp. Fig. 2Dii). Taken together these results show that while Pax3 and Pax7 have previously been mainly demonstrated to act as transcriptional activators during embryogenesis (Budry et al., 2012; McKinnell et al., 2008; Relaix et al., 2003), in the neural tube these TFs contribute to neural tube patterning through transcriptional repression. It is also noteworthy that *Dbx1* expression is hardly ever detected and only occurs at very low levels in the somites of wild-type embryos (Fig. 2Hiii) but that it is strongly induced in $Pax3^{PAX3A/+}$ embryos (Fig. 2Hiv); therefore suggesting that Pax3-mediated repression of Dbx1 also occurs in Pax3 dependent myogenic lineages. This hints that our work may prove relevant in a spectrum of tissue types.

Dbx1 locus harbours several Pax responsive *cis*-regulatory modules

We next decided to evaluate whether Pax3 and Pax7 could directly control *Dbx1* transcription by acting at the level of *Dbx1* associated *cis*-regulatory modules (CRM). To identify these CRMs, we first compared the *Dbx1 loci* and the surrounding 10kb intergenic regions of several vertebrate species ranging from human to fugu. This approach revealed the existence of 5 blocks of conservation: three of them located within 4.2kb upstream of the *Dbx1* transcription start site (CRM1, CRM2, CRM3); the other two within the second intron (iCRM1, iCRM2) (Fig. 3A). In addition, ENCODE epigenetic data on the neural tube of GD11.5 or GD12.5 mouse embryos further supports the functionality of these CRMs (see Material and Methods). Notably, DNase hypersensitivity and histone modification H3K27ac, whose combined occurrence defines active enhancers, are both present at the level of the two iCRMs. Additionally, the H3K4me1 epigenetic mark of active and/or poised enhancers is detected at iCRM2, CRM2 and CRM3 (Fig. 3A). Furthermore, in ESC-derived neuroprogenitors, binding events for Sox2 and Sox3, two TFs involved in *Dbx1* regulation (Rogers et al., 2014), have been identified within the Dbx1 iCRM (Fig. 3A)(Bergsland et al., 2012). Finally, the 3 intergenic CRMs are located within a 5.7kb region capable of driving the expression of reporter transgenes within the intermediate spinal cord of mouse and chick embryos (Dyck et al., 2012; Lu et al., 1996; Matise et al., 1999; Thelié et al., 2015); while CRM3 on its own has also been reported to be active in the intermediate neural tube of chick embryos (Oosterveen et al., 2012). In order to test the ability of the candidate CRMs to respond to Pax3/7 individually or collectively, we generated reporter constructs and tested their activity in the neural tube of chick embryos 24 and 36 hours after their electroporation at stage HH10-11 (Fig. 3B,C, data not shown). Amongst the three intergenic CRMs, only CRM3 displays any activity, as previously described (Oosterveen et al., 2012)(Fig. 3Bi-iii, C), yet, the expression of the reporter protein driven by this element is weak, as it was detected in only 4 embryos out of 14. In addition, it is

not restricted to the Dbx1^{+} domain (Fig. 3Biii). Likewise, the CRM4.8kb module, which contains CRM1, 2 and 3 (Fig. 3A) is poorly able to induce gene expression in the neural tube of chick embryos (Fig. 3Biv); only 4 embryos out of 21 display any β-Galactosidase expression. When detected, the activity of this module is not restricted to the Dbx1^{+} domain but encompasses the entire dorsal neural tube (Fig. 3Biv, C). This is consistent with previously identified ectopic dorsal activity of a 5.7kb CRM in the neural tube of mouse embryos (Lu et al., 1996; Matise et al., 1999) and indicates that the intergenic CRMs may not be the main drivers of the restriction of *Dbx1* expression to the intermediate spinal cord. We next evaluated the ability of the two intronic CRMs to induce gene expression using a construct, containing both modules and the region between them, termed iCRM (Fig. 3A). The iCRM construct systematically promotes β-Galactosidase expression in the neural tube 24hpe and 36hpe. The overall levels of this reporter are weak, but expression is always found exclusively within the Dbx1 domain (Fig. 3Bv-v'', C and data not shown). Hence the iCRM contains all the necessary information to recapitulate Dbx1 induction and D-V restriction. Strengthening this argument, adding the iCRM to the CRM4.8kb was sufficient to abolish the CRM4.8kb ectopic dorsal activity and promote strong *LacZ* gene expression in the Dbx1^{+} domain alone, as assessed at 36hpe (Fig. 3Bvi). It is worth mentioning that *Dbx1 LacZ* KI reporter mice have previously been generated, where *LacZ* replaces the four exons and three introns (including the iCRM) of *Dbx1* (Pierani et al., 2001). Interestingly, β-Galactosidase expression matches with that of Dbx1 in these animals, thus, the iCRM is unlikely to be the only module responsible for *Dbx1* gene regulation in the neural tube. It is tempting to hypothesise that it behaves as a shadow enhancer providing robustness to Dbx1 transcription.

We next used *in silico* approaches to evaluate whether these CRMs contain putative Pax3/7 binding sites. We first identified the most phylogenetically conserved 15 base pair long DNA motifs contained in these CRMs using MEME (cf. Materials and Methods). Then, we searched

within the extracted motifs for putative Pax binding sites using the TOMTOM database, or using FIMO and Pax3- and Pax7-specific position weight matrices (PWMs)(Supp. Fig. 3A), as Pax binding domains have some level of family member specificity and Pax3 and Pax7 PWMs are not defined in TOMTOM databases (Jolma et al., 2013; Mayran et al., 2015). These were either previously defined by HT-SELEX (Jolma et al., 2013) or Pax3 and Pax7 ChIP-Seq performed in myoblasts (Soleimani et al., 2012). These two methods identified putative Pax3 and Pax7 binding sites in iCRM, CRM2 and CRM3 (Fig. 3Axii). Further supporting this, Pax7 has been shown to be able to bind to the 2 sites identified in iCRM and one of the sites located in CRM3 in myoblasts (Soleimani et al., 2012) (Fig. 3Axi). Probing this further, we noted that the electroporation of either Pax3 or Pax7 induces significant changes in the activity of iCRM, CRM4.8kb and CRM3 in the neural tube of chick embryos 24hpe (Fig. 3D, Supp. Fig. 3B, data not shown); promoting the activity of the latter and repressing that of the other two. These results provide one possible explanation for why the intergenic CRM3 or CRM4.8Kb harbour ectopic activity in the dorsal neural tube which expresses Pax3 and Pax7, while the iCRM is restricted to the intermediate domain. Furthermore, electroporation of PAX3A stimulates the activity of all the CRMs (Fig. 3D, Supp. Fig. 3B). Notably, its impact was stronger on that of the iCRM than on all other constructs. Conversely, electroporation of Pax3R inhibits the activity of iCRM, CRM4.8kb and CRM3 (data not shown). Altogether, these results support the idea that Pax3 and Pax7 directly regulate Dbx1 by modulating the activity of several CRMs, repressing transcription through iCRM, CRM1 and CRM2, and activating it through CRM3.

Pax3 and Pax7 mediated *Dbx1* regulation involves an additional genetic interaction

The progressive attenuation of *Dbx1* expression in the dKO embryos observed between GD10.5 and GD11.5 (compare Fig. 2C to Supp. Fig. 2B) could not be solely explained by the repression of *Dbx1* locus activity by Pax3 and Pax7. We, thus, looked for candidate TFs that would be

regulated by Pax3 and Pax7 and whose activity would impact onto *Dbx1* expression. Prdm12, a p1 fate determinant known to repress Dbx1 expression, as well as the activity of CRM4.8kb in chick embryos (Kinameri et al., 2008; Thelié et al., 2015), appeared an obvious candidate. We analysed its expression by *in situ* hybridisation in GD11.5 Pax3 and Pax7 mutant embryos (Fig. 4B). In single mutants for Pax3 and Pax7, we did not detect any defects in the expression profile of this TF (Fig. 4Bii). In contrast, in dKO embryos, the *Prdm12* expression domain is dorsally enlarged and overlaps with the extended *Dbx1* domain (Fig. 4Biv, Supp. Fig. 2Di). *Prdm12* is also ectopically induced in $Pax3^{-/-};Pax7^{+/-}$ embryos, but to a much lesser extent than in the dKO embryos (Fig. 4Biii-iv). These results indicate that Pax3 and Pax7 are both required to position of the dorsal boundary of *Prdm12* domain. To assess whether this is mediated by a repressive activity of the Pax TFs, we assessed for *Prdm12* in embryos carrying Pax3A and Pax3R variants (Fig. 4Bv-vii). Expression of the latter Pax3 variant has no effect on *Prdm12* expression (Fig. 4Bvii), while the dominant active form of Pax3 induces ectopic dorsal expression of Prdm12 (Fig. 4Bv). Taken together these results indicated that Pax3 and Pax7 repress *Prdm12* expression. As Prdm12 is a repressor of Dbx1 (Thelié et al., 2015), Pax3/7 mediated Prdm12 repression provides an explanation for why the removal of Pax3 and Pax7 results in the attenuation of *Dbx1* expression. This also shows that the regulation of Dbx1 by Pax3 and Pax7 is complex and includes both positive and negative components. The latter is a direct regulation while the former is indirect. It is tempting to hypothesise that this incoherent regulatory network formed by Pax3/7, Dbx1 and Prdm12 explains, in parts, why the levels of Pax3 and Pax7 repression play such a key role during the generation of intermediate neural cell fates (Fig. 4C, Alon, 2007; Balaskas et al., 2012).

Conclusion/Discussion

First of all, this paper provides strong evidence that progenitor cells of the intermediate neural tube are able to sense and interprete the dose and the levels of Pax3 and Pax7 transcriptional activity, as shown by the progressively more dorsal fates seen upon increasing Pax levels (Fig. 1). This is highly reminiscent of the mode of interpretation of TF-based morphogen gradients (Rushlow and Shvartsman, 2012). Our data further suggest that in the case of Pax3 and Pax7, graded activity throughout the D-V axis of the intermediate neural tube is likely to be established thanks to the temporal restriction of their expression profiles. It is also tempting to hypothesise that Pax3 and Pax7 diffuse ventrally over a short range and thus form a gradient sufficient to provide robustness to pattern formation, as proven for Pax6, another member of the Pax family (Prochiantz and Di Nardo, 2015; Quiñinao et al., 2015). Second, we have highlighted the importance of the repressive transcriptional activity of Pax3 and Pax7 in this process, especially for the spatial restriction and numbering of the V0 and V1 IN. This contrasts with Pax3/7 mediated cell fate specification in other tissues, which is rather based on transcriptional activation (Budry et al., 2012; McKinnell et al., 2008; Relaix et al., 2003). Whether this is due to differential usage of their DNA binding domains or specific protein partners remains to be studied (Mayran et al., 2015). Finally, our study has identified several of the genetic interactions of the gene network by which Pax3 and Pax7 regulate the organisation of cell fates within the intermediate spinal cord. Dbx1 displays a central position in this network and we have demonstrated that it receives both a likely direct negative input and an indirect positive input from Pax3 and Pax7 (Fig. 4C). On the one hand, we provide several pieces of evidence for the direct repression of Dbx1 by Pax3 and Pax7. We have shown that *Dbx1* expression displays a dose response to levels of Pax3 and Pax7 activity and that several Dbx1 *cis*-regulatory elements are responsive to the modulation of Pax3 and Pax7 transcriptional activity. Not only do these harbour putative Pax3 and Pax7 binding sites, but physical

interactions between Pax3 and Pax7 and two of these CRMs have also been observed in myoblast cells (Soleimani et al., 2012). Importantly, our data indicate that the negative input of Pax3 and Pax7 on Dbx1 plays an essential role in positioning the dorsal border of the Dbx1 expression domain. As we and others have demonstrated that Dbx1 promotes V0 fate by inhibiting the expression of determinants of the adjacent dI6 and V1 cell populations ((Karaz et al., 2016; Lanuza et al., 2004; Pierani et al., 2001), Fig. 4A), this genetic interaction provides a fairly simple mechanism for how the Pax TFs impact on the size of V0 and dI6 IN populations (Karaz et al., 2016; Lanuza et al., 2004; Pierani et al., 2001), Fig. 1, Fig. 4A, Supp. Fig. 1E,F). On the other hand, we have shown that Pax3 and Pax7 repress Prdm12, a known repressor of Dbx1 (Thelié et al., 2015). Interestingly, this regulatory loop provides a molecular explanation for the massive ectopic dorsal generation of V1 cells in Pax3 and Pax7 double mutants described twenty years ago ((Mansouri and Gruss, 1998), Fig. 1). Furthermore, it supports a model whereby D-V progenitor pool determinants not only repress genes expressed in adjacent pools, but also expressed in pools located further way (e.g. (Kutejova et al., 2016)). Altogether, our paper supports the ideas that (i) the patterning potential of TFs is extended by the ability of progenitors to read and extrapolate discrete levels of TF activity, that (ii) these levels can be modulated thanks to genetic redundancy induced by gene duplication and/or dynamics in their expression profiles and that (iii) the generation of the diversity of progenitor pools in the developing neural tube might not be mediated by multiple binary cell fate choices between adjacent progenitor pools but by the active repression of several alternative fates.

Acknowledgments

We deeply thank C. Birchmeier and T. Müller for antibodies as well as M.A. Rudnicki and P. Gruss for providing plasmids. We also thank the ImagoSeine core facility of Institut Jacques

Monod, a member of France-BioImaging (ANR-10-INBS-04) and certified IBiSA. We acknowledge the ENCODE consortium and B. Ren (UCSD) and Z. Weng (Umass) laboratories for the generation of the reference epigenome for embryonic mouse neural tube data. We are grateful to the biological service staff of the CDTA and Buffon animal housing for help with the mouse colonies. FC and VR are INSERM researchers. Work in the lab of VR was supported by CNRS/INSERM ATIP-AVENIR program. Studies in the lab of AP is funded by Agence Nationale pour la Recherche (ANR-15-CE16-0003-01) and Fondation pour la Recherche Médicale (INE20060306503 and «Equipe FRM DEQ 20130326521»). This work was supported by funding to FR from Association Française contre les Myopathies (AFM) via TRANSLAMUSCLE (PROJECT 19507), Labex REVIVE (ANR-10-LABX-73), Fondation pour la Recherche Médicale (FRM; Grant FDT20130928236), Agence Nationale pour la Recherche (ANR) grant Satnet (ANR-15-CE13-0011-01) and bone-muscle-repair (ANR-13-BSV1-0011-02).

References

Alon, U., 2007. Network motifs: theory and experimental approaches. Nat Rev Genet 8, 450–461.

Armant, O., März, M., Schmidt, R., Ferg, M., Diotel, N., Ertzer, R., Bryne, J.C., Yang, L., Baader, I., Reischl, M., Legradi, J., Mikut, R., Stemple, D., Ijcken, W. Van, van der Sloot, A., Lenhard, B., Strähle, U., Rastegar, S., 2013. Genome-wide, whole mount in situ analysis of transcriptional regulators in zebrafish embryos. Dev. Biol. 380, 351–62. doi:10.1016/j.ydbio.2013.05.006

Bailey, P.J., Klos, J.M., Andersson, E., Karlén, M., Källström, M., Ponjavic, J., Muhr, J., Lenhard, B., Sandelin, A., Ericson, J., Karlen, M., Kallstrom, M., 2006. A global genomic transcriptional code associated with CNS-expressed genes. Exp Cell Res 312, 3108–3119.

468 doi:10.1016/j.yexcr.2006.06.017
469 Bajard, L., Relaix, F., Lagha, M., Rocancourt, D., Daubas, P., Buckingham, M.E., 2006. A
470 novel genetic hierarchy functions during hypaxial myogenesis: Pax3 directly activates
471 Myf5 in muscle progenitor cells in the limb. Genes Dev. 20, 2450–64.
472 doi:10.1101/gad.382806
473 Balaskas, N., Ribeiro, A., Panovska, J., Dessaud, E., Sasai, N., Page, K.M., Briscoe, J., Ribes,
474 V., 2012. Gene regulatory logic for reading the Sonic Hedgehog signaling gradient in the
475 vertebrate neural tube. Cell 148, 273–284. doi:10.1016/j.cell.2011.10.047
476 Bergsland, M., Ramskold, D., Zaouter, C., Klum, S., Sandberg, R., Muhr, J., 2012. Sequentially
477 acting Sox transcription factors in neural lineage development. Genes Dev 25, 2453–2464.
478 Borromeo, M.D., Meredith, D.M., Castro, D.S., Chang, J.C., Tung, K.-C., Guillemot, F.,
479 Johnson, J.E., 2014. A transcription factor network specifying inhibitory versus excitatory
480 neurons in the dorsal spinal cord. Development 2812, 2803–2812.
481 doi:10.1242/dev.105866
482 Briscoe, J., Pierani, A., Jessell, T.M., Ericson, J., 2000. A homeodomain protein code specifies
483 progenitor cell identity and neuronal fate in the ventral neural tube. Cell 101, 435–445.
484 Budry, L., Balsalobre, A., Gauthier, Y., Khetchoumian, K., L'Honoré, A., Vallette, S., Brue,
485 T., Figarella-Branger, D., Meij, B., Drouin, J., L'Honore, A., Vallette, S., Brue, T.,
486 Figarella-Branger, D., Meij, B., Drouin, J., 2012. The selector gene Pax7 dictates alternate
487 pituitary cell fates through its pioneer action on chromatin remodeling. Genes Dev 26,
488 2299–2310. doi:10.1101/gad.200436.112
489 Del Corral, R.D., Storey, K.G., 2004. Opposing FGF and retinoid pathways: A signalling switch
490 that controls differentiation and patterning onset in the extending vertebrate body axis.
491 BioEssays 26, 857–869. doi:10.1002/bies.20080
492 Dessaud, E., Ribes, V., Balaskas, N., Yang, L.L., Pierani, A., Kicheva, A., Novitch, B.G.,

493 Briscoe, J., Sasai, N., 2010. Dynamic assignment and maintenance of positional identity
494 in the ventral neural tube by the morphogen sonic hedgehog. PLoS Biol 8, e1000382.
495 Drouin, J., 2014. Pioneer transcription factors in cell fate specification. Mol. Endocrinol. 28,
496 me20141084. doi:10.1210/me.2014-1084
497 Dyck, J., Lanuza, G.M., Gosgnach, S., 2012. Functional characterization of dI6 interneurons in
498 the neonatal mouse spinal cord 3256–3266. doi:10.1152/jn.01132.2011
499 Epstein, D.J., Vekemans, M., Gros, P., 1991. Splotch (Sp2H), a mutation affecting development
500 of the mouse neural tube, shows a deletion within the paired homeodomain of Pax-3. Cell
501 67, 767–774.
502 Goulding, M.D., Chalepakis, G., Deutsch, U., Erselius, J.R., Gruss, P., 1991. Pax-3, a novel
503 murine DNA binding protein expressed during early neurogenesis. EMBO J. 10, 1135–
504 1147.
505 Jolma, A., Yan, J., Whitington, T., Toivonen, J., Nitta, K.R., Rastas, P., Morgunova, E., Enge,
506 M., Taipale, M., Wei, G., Palin, K., Vaquerizas, J.M., Vincentelli, R., Luscombe, N.M.,
507 Hughes, T.R., Lemaire, P., Ukkonen, E., Kivioja, T., Taipale, J., 2013. DNA-binding
508 specificities of human transcription factors. Cell 152, 327–339.
509 doi:10.1016/j.cell.2012.12.009
510 Jostes, B., Walther, C., Gruss, P., 1990. The murine paired box gene, Pax7, is expressed
511 specifically during the development of the nervous and muscular system. Mech Dev 33,
512 27–37.
513 Karaz, S., Courgeon, M., Lepetit, H., Bruno, E., Pannone, R., Tarallo, A., Thouzé, F., Kerner,
514 P., Vervoort, M., Causeret, F., Pierani, A., Onofrio, G.D., 2016. Neuronal fate
515 specification by the Dbx1 transcription factor is linked to the evolutionary acquisition of
516 a novel functional domain. Evodevo 1–13. doi:10.1186/s13227-016-0055-5
517 Kinameri, E., Inoue, T., Aruga, J., Imayoshi, I., Kageyama, R., Shimogori, T., Moore, A.W.,

518 2008. Prdm proto-oncogene transcription factor family expression and interaction with the
519 Notch-Hes pathway in mouse neurogenesis. PLoS One 3, 1–10.
520 doi:10.1371/journal.pone.0003859
521 Kutejova, E., Sasai, N., Shah, A., Gouti, M., Briscoe, J., 2016. Neural Progenitors Adopt
522 Specific Identities by Directly Repressing All Alternative Progenitor Transcriptional
523 Programs. Dev. Cell 1–15. doi:10.1016/j.devcel.2016.02.013
524 Lai, H.C., Seal, R.P., Johnson, J.E., 2016. Making sense out of spinal cord somatosensory
525 development. Development 143, 3434–3448. doi:10.1242/dev.139592
526 Lallemand, Y., Luria, V., Haffner-Krausz, R., Lonai, P., 1998. Maternally expressed PGK-Cre
527 transgene as a tool for early and uniform activation of the Cre site-specific recombinase.
528 Transgenic Res 7, 105–112.
529 Lanuza, G.M., Gosgnach, S., Pierani, A., Jessell, T.M., Goulding, M., 2004. Genetic
530 identification of spinal interneurons that coordinate left-right locomotor activity necessary
531 for walking movements. Neuron 42, 375–86.
532 Lu, D.C., Niu, T., Alaynick, W.A., 2015. Molecular and cellular development of spinal cord
533 locomotor circuitry 8, 1–18. doi:10.3389/fnmol.2015.00025
534 Lu, S., Shashikant, C.S., Ruddle, F.H., 1996. Separate cis-acting elements determine the
535 expression of mouse Dbx gene in multiple spatial domains of the central nervous system.
536 Mech. Dev. 58, 193–202.
537 Mansouri, A., Gruss, P., 1998. Pax3 and Pax7 are expressed in commissural neurons and restrict
538 ventral neuronal identity in the spinal cord. Mech Dev 78, 171–178.
539 Mansouri, A., Stoykova, A., Torres, M., Gruss, P., 1996. Dysgenesis of cephalic neural crest
540 derivatives in Pax7-/- mutant mice. Development 122, 831–838.
541 Matise, M.P., Lustig, M., Sakurai, T., Grumet, M., Joyner, A.L., 1999. Ventral midline cells
542 are required for the local control of commissural axon guidance in the mouse spinal cord

543 3659, 3649–3659.
544 Mayran, A., Pelletier, A., Drouin, J., 2015. Pax factors in transcription and epigenetic
545 remodelling. Semin. Cell Dev. Biol. 1–10. doi:10.1016/j.semcdb.2015.07.007
546 Mazzoni, E.O., Mahony, S., Closser, M., Morrison, C. a, Nedelec, S., Williams, D.J., An, D.,
547 Gifford, D.K., Wichterle, H., 2013. Synergistic binding of transcription factors to cell-
548 specific enhancers programs motor neuron identity. Nat. Neurosci. 16, 1219–27.
549 doi:10.1038/nn.3467
550 McKinnell, I.W., Ishibashi, J., Le Grand, F., Punch, V.G., Addicks, G.C., Greenblatt, J.F.,
551 Dilworth, F.J., Rudnicki, M.A., 2008. Pax7 activates myogenic genes by recruitment of a
552 histone methyltransferase complex. Nat Cell Biol 10, 77–84.
553 Megason, S.G., McMahon, A.P., 2002. A mitogen gradient of dorsal midline Wnts organizes
554 growth in the CNS. Development 129, 2087–2098.
555 Moore, S., Ribes, V., Terriente, J., Wilkinson, D., Relaix, F., Briscoe, J., 2013. Distinct
556 regulatory mechanisms act to establish and maintain Pax3 expression in the developing
557 neural tube. PLoS Genet. 9, e1003811. doi:10.1371/journal.pgen.1003811
558 Muhr, J., Andersson, E., Persson, M., Jessell, T.M., Ericson, J., 2001. Groucho-mediated
559 transcriptional repression establishes progenitor cell pattern and neuronal fate in the
560 ventral neural tube. Cell 104, 861–873.
561 Nakazaki, H., Reddy, A.C., Mania-Farnell, B.L., Shen, Y.-W.W., Ichi, S., McCabe, C., George,
562 D., McLone, D.G., Tomita, T., Mayanil, C.S.K.S.K., 2008. Key basic helix-loop-helix
563 transcription factor genes Hes1 and Ngn2 are regulated by Pax3 during mouse embryonic
564 development. Dev Biol 316, 510–523. doi:10.1016/j.ydbio.2008.01.008
565 Oosterveen, T., Kurdija, S., Alekseenko, Z., Uhde, C.W., Bergsland, M., Sandberg, M.,
566 Andersson, E., Dias, J.M., Muhr, J., Ericson, J., 2012. Mechanistic Differences in the
567 Transcriptional Interpretation of Local and Long-Range Shh Morphogen Signaling. Dev.

568 Cell 23, 1006–1019. doi:10.1016/j.devcel.2012.09.015
569 Pierani, A., Brenner-Morton, S., Chiang, C., Jessell, T.M., 1999. A Sonic Hedgehog–
570 Independent, Retinoid-Activated Pathway of Neurogenesis in the Ventral Spinal Cord.
571 Cell 97, 903–915. doi:10.1016/S0092-8674(00)80802-8
572 Pierani, A., Sunshine, M.J., Littman, D.R., Goulding, M., Jessell, T.M., 2001. Control of
573 Interneuron Fate in the Developing Spinal Cord by the Progenitor Homeodomain Protein
574 Dbx1 29, 367–384.
575 Prochiantz, A., Di Nardo, A.A., 2015. Homeoprotein Signaling in the Developing and Adult
576 Nervous System. Neuron 85, 911–925. doi:10.1016/j.neuron.2015.01.019
577 Quiñinao, C., Prochiantz, A., Touboul, J., 2015. Local homeoprotein diffusion can stabilize
578 boundaries generated by graded positional cues. Development 142, 1860–8.
579 doi:10.1242/dev.113688
580 Relaix, F., Polimeni, M., Rocancourt, D., Ponzetto, C., Schafer, B.W., Buckingham, M.,
581 Schäfer, B.W., 2003. The transcriptional activator PAX3-FKHR rescues the defects of
582 Pax3 mutant mice but induces a myogenic gain-of-function phenotype with ligand-
583 independent activation of Met signaling in vivo. Genes Dev 17, 2950–2965.
584 doi:10.1101/gad.281203
585 Relaix, F., Rocancourt, D., Mansouri, A., Buckingham, M., 2005. A Pax3/Pax7-dependent
586 population of skeletal muscle progenitor cells. Nature 435, 948–953.
587 doi:10.1038/nature03594
588 Rogers, N., McAninch, D., Thomas, P., 2014. Dbx1 Is a Direct Target of SOX3 in the Spinal
589 Cord. PLoS One 9, e95356. doi:10.1371/journal.pone.0095356
590 Rushlow, C.A., Shvartsman, S.Y., 2012. Temporal dynamics, spatial range, and transcriptional
591 interpretation of the Dorsal morphogen gradient. Curr. Opin. Genet. Dev. 22, 542–6.
592 doi:10.1016/j.gde.2012.08.005

593 Soleimani, V.D., Punch, V.G., Kawabe, Y.I., Jones, A.E., Palidwor, G. a., Porter, C.J., Cross,
594 J.W., Carvajal, J.J., Kockx, C.E.M., van IJcken, W.F.J., Perkins, T.J., Rigby, P.W.J.,
595 Grosveld, F., Rudnicki, M. a., 2012. Transcriptional Dominance of Pax7 in Adult
596 Myogenesis Is Due to High-Affinity Recognition of Homeodomain Motifs-supp. Dev.
597 Cell 22, 1208–1220. doi:10.1016/j.devcel.2012.03.014
598 Spitz, F., Furlong, E.E., 2012. Transcription factors: from enhancer binding to developmental
599 control. Nat Rev Genet 13, 613–626.
600 Thelié, A., Desiderio, S., Hanotel, J., Quigley, I., Driessche, B. Van, Rodari, A., Borromeo,
601 M.D., Kricha, S., Lahaye, F., Croce, J., Cerda-moya, G., Bolle, B., Lewis, K.E., Sander,
602 M., Pierani, A., Schubert, M., Johnson, J.E., Kintner, C.R., Pieler, T., Lint, C. Van,
603 Henningfeld, K.A., Bellefroid, E.J., Campenhout, C. Van, 2015. Prdm12 specifies V1
604 interneurons through cross-repressive interactions with Dbx1 and Nkx6 genes in Xenopus
605 3416–3428. doi:10.1242/dev.121871
606 Yamada, T., Pfaff, S.L., Edlund, T., Jessell, T.M., 1993. Control of cell pattern in the neural
607 tube: motor neuron induction by diffusible factors from notochord and floor plate. Cell 73,
608 673–86.
609 Yee, S., Rigby, P.J., Hill, M., Uk, N.W., 1993. The regulation of myogenin gene expression
610 duringthe embryonic development of tile mouse 1277–1289.
611

612 # Figure legends

613 **Fig. 1: Pax3 and Pax7 regulate the production of interneuron populations in the**
614 **intermediate part of the spinal cord**

615 **A.** Immunostaining for Lbx1, AP2α, Brn3a to identify dI6 IN **(i-vii)**, Pax2, Lbx1 and Evx1 to
616 reveal $V0_D$ IN (**viii-xiv**) and FoxD3 and Evx1 to label $V0_{VCG}$ and V1 IN populations,

617 respectively (**xv-xxi**) performed on brachial transverse sections of GD11.5 mouse embryos of
618 the indicated genotype. In **ii**, Ap2α is not labelled. In **ix-xi** Evx1 is not marked. Scale bars:
619 50µm. Dashed lines delineate the pools of interneuron subtypes. Asterisks in **iv** and **vii** mark
620 the lack of dI6 cells. In **xii** and **xiii**, V0* indicates that the $V0_D$ and $V0_{VCG}$ are intermingled.
621 Arrowheads in **xvii** and **xviii** point at ectopic V1 cells and limited V0 cells, respectively. **B.**
622 Quantification of the number of each neuronal subtype in GD11.5 mouse embryos with the
623 indicated genotype (dI6 IN are $Lbx1^+/Ap2\alpha^-/Brn3a^-$, $V0_D$ IN are $Pax2^+/Lbx1^-/Evx1^-$, $V0_{VCG}$ IN
624 are $Evx1^+$, V1 IN are $FoxD3^+$). Red bars denote the mean values. Mann–Whitney U test p-
625 values are represented as follows: *: p≤0.05; **: p≤0.01; ***: p≤0.001; ****: p≤0.0001. **C.**
626 Representation of the pools of progenitor cells in the spinal cord and the neuronal populations
627 they give rise to. The dI6, V0 and V1 populations are highlighted and the expression of TFs
628 that allows their determination are shown. The distribution of these populations in the
629 Pax3/Pax7 mutant backgrounds that were analysed are summarised.
630
631 **Fig. 2: Pax3 and Pax7 repressive activity positions the dorsal boundary of *Dbx1* expression**
632 **A.** Immunostaining for Dbx1/β-Galactosidase/GFP in thoracic transverse sections of GD11.5
633 $Pax3^{GFP/+;}$ $Pax7^{LacZ/+}$ embryos (**i-i''**) and Dbx1/Pax3 at brachial level of GD10.5 wild-type
634 embryo (**ii-ii'**). Quantification of the proportion of $Dbx1^+$ cells expressing Pax3 or Pax3 lineage
635 marker GFP at GD11.5 in thoracic transverse sections (**iii**, mean±s.e.m, n=4 embryos). **B.**
636 Schematics showing the temporal dynamics of Pax3, Pax7, Dbx1 and Prdm12 expression
637 profiles in the dp6, p0 and p1 spinal progenitor pools and the neurons they will generate. **C-H.**
638 *In situ* hybridisation for *Dbx1* (**Ci-ii; Ei-iii; Fi-iv, Hi-iv**) and immunolabelling of Dbx1 (**Di-iv,**
639 **Gi-iv**) in brachial transverse sections of either mouse embryos of the indicated stage and
640 genotype (**C, D, F-H**) or in chick embryos 24hpe with the indicated plasmid **(E)**. For the latter
641 samples, nuclei were also labelled with DAPI and the electroporated cells with

immunofluorescent labelling of GFP (**Ei', ii', iii'**). Graphs in **Ciii** and **Fv** display the absolute D-V position of the *Dbx1* expression domain from the floor plate in μm (mean ± s.e.m on 6 sections for each embryo subtype). Graphs in **Dv and Gv** show the number of $Dbx1^+$ cells per transverse section at brachial level in GD11.5 embryos of the indicated genotype. The mean value is indicated by the red bar. Mann–Whitney U test p-values are represented as follows: *: $p \leq 0.05$; **: $p \leq 0.01$; ***: $p \leq 0.001$; ****: $p \leq 0.0001$. Scale bars: 50 μm.

Fig. 3: Dbx1 CRMs are responsive to Pax3 and Pax7 activity

A. Schematics displaying the *Dbx1* locus (**i**), regions of conservation across 60 species of vertebrates (**ii**) and putative *cis*-regulatory modules (**iii**). iCRM is located in *Dbx1* intron 2, while CRM1-3 are located in a 4.8kb region upstream the *Dbx1* TSS (CRM4.8kb) and all show high sequence conservation. DNase-seq (**iv**), H3K27ac ChIPseq (**v**) and enhancer predictions (**vi**) in GD11.5 neural tube (NT) support the potential enhancer role of iCRM. H3K4me1 ChIPseq signal at GD11.5 (**vii**) and GD12.5 (**viii**) is enriched in iCRM and in CRM2 and CRM3 within the CRM4.8kb. Moreover, the iCRM region shows Sox2 (**ix**) and Sox3 (**x**) binding events. Pax7 binding events in muscle cells (**xi**) coincide with the iCRM and CRM4.8kb putative regulatory regions, which also harbour *in silico* predicted Pax3/7 binding sites (**xii**). **B.** Immunostaining for Dbx1/β-Galactosidase/GFP in chick embryos 24hpe with *pCIG* and the indicated reporter constructs carrying *Dbx1* CRMs. Scale bars: 50 μm. **C-D.** Heatmaps display the levels of β–Galactosidase expression normalised to that of GFP along the D-V axis of the neural tube of chick embryos 24hpe with the indicated *Dbx1* CRM reporters and either *pCIG* (C and columns 1 in D), *Pax3-GFP* (columns 2 in D) or *PAX3A-GFP* (columns 3 in D).

Fig. 4: Characterisation of genetic interactions within the Pax3 and Pax7 linked gene network

A. Immunostaining for Lbx1, Pax3, Pax7 and GFP on chick embryos 40hpe with *mDbx1-IRES-GFP* constructs, indicating that Dbx1 overexpression is sufficient to inhibit the generation of $Lbx1^+$ neurons (**i, i'**), shut down Pax3 (**ii, ii'**), and decrease the levels of Pax7 expression (**iii, iii'**). Scale bars = 50 μm. **B.** *In situ* hybridisation for *Prdm12* in brachial transverse sections of GD11.5 (**i-v**) and GD10.5 (**vi, vii**) mouse embryos of the indicated genotype. Graphs below the ISH panels display the absolute D-V position of the *Dbx1* expression domain (pink, the striped domain indicates low levels of expression) and the distribution profile of *Prdm12* mRNA (pale blue) along the D-V axis (y axis gives the D-V position from the floor plate in μm, mean ± s.e.m on more than 6 sections for each embryo subtype). **C.** Schematics representing the regulatory interactions within the gene network that is responsible for Pax3 and Pax7 mediated Dbx1 gene regulation; (a) refers to Fig 2C & E, (b) repression in dashed line as the repression of Pax7 is partial, see Fig. 4Aii,iii, (c) refers to Fig. 4B, (d) refers to (Thelié et al., 2015).

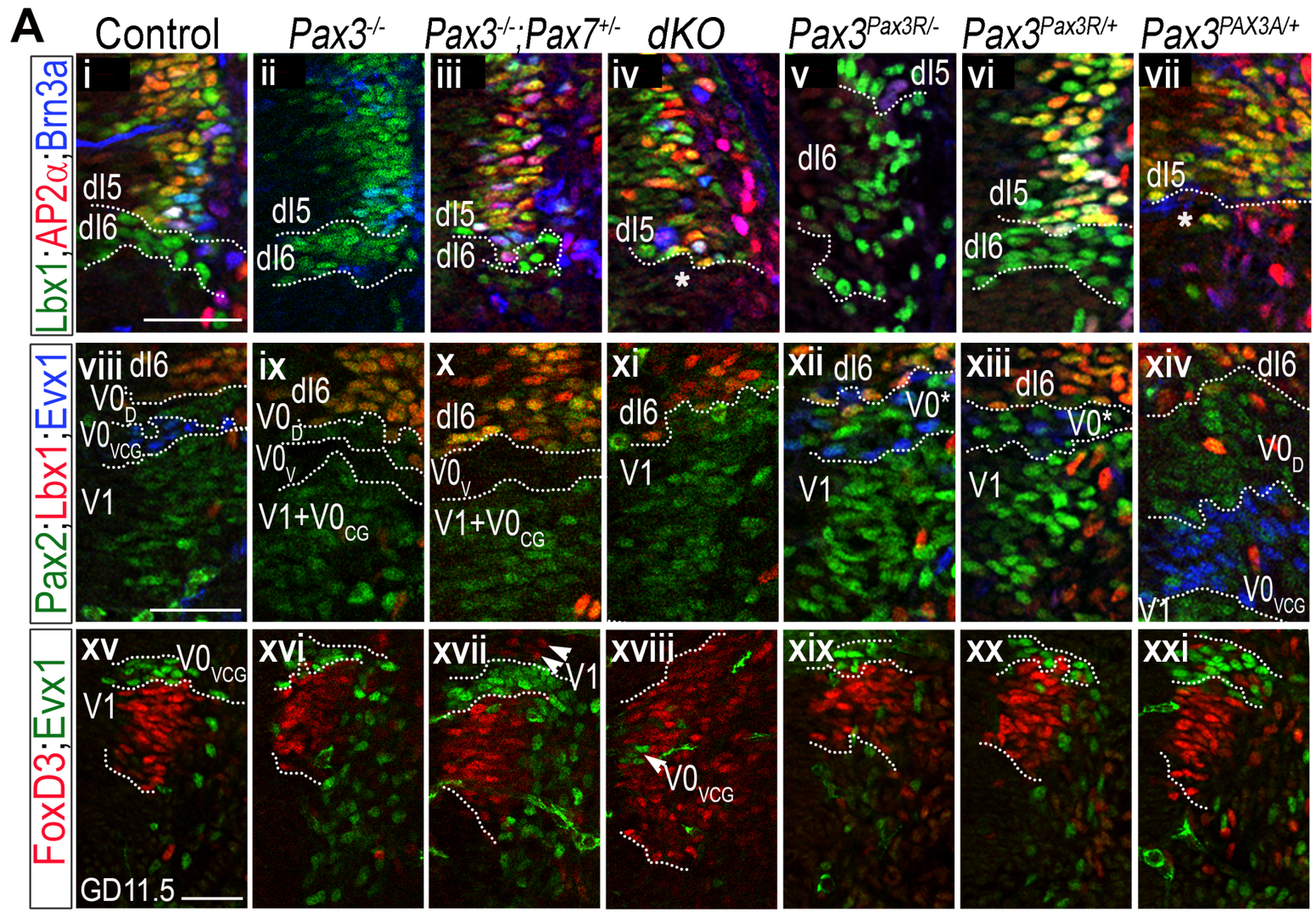

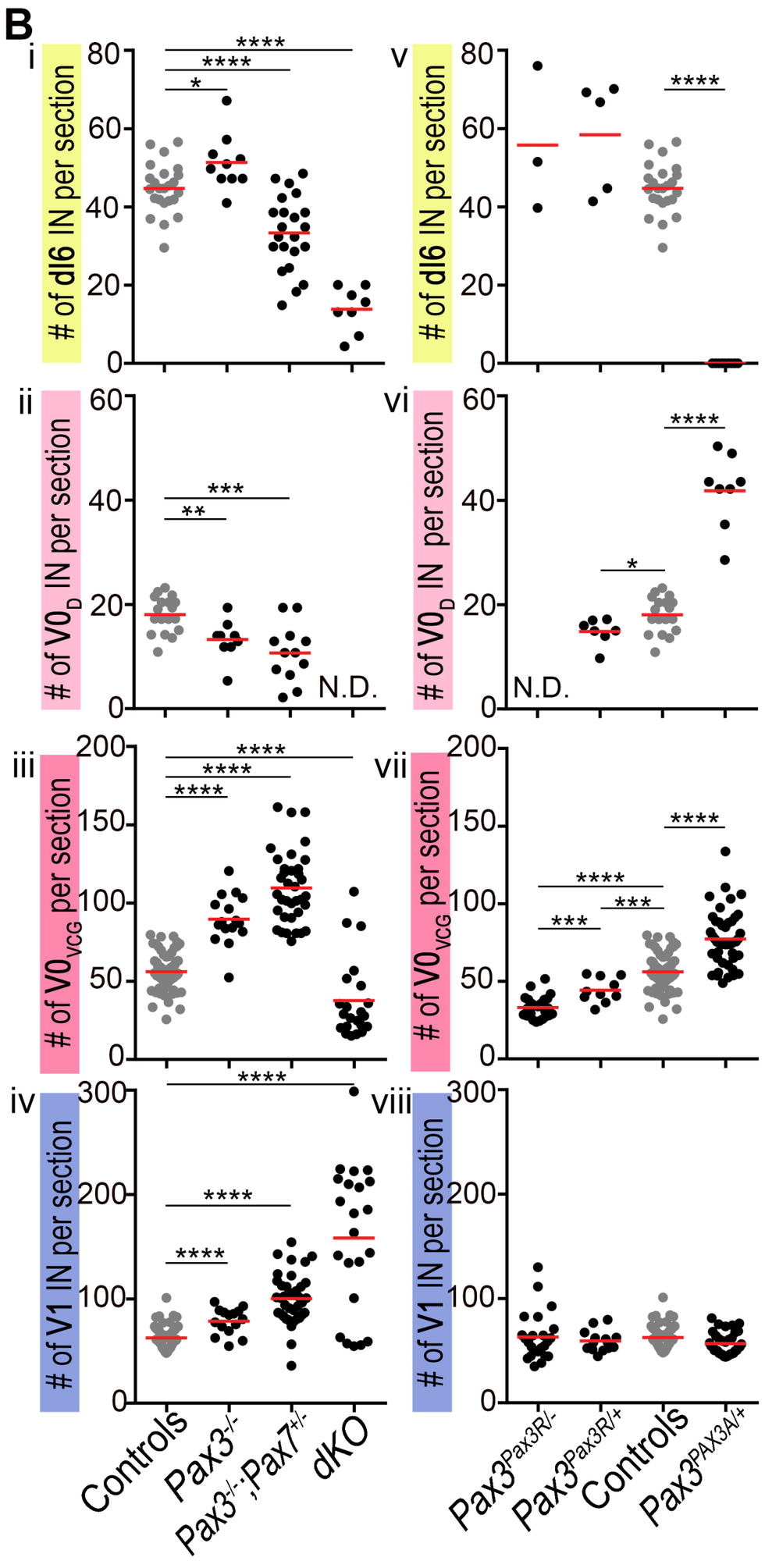

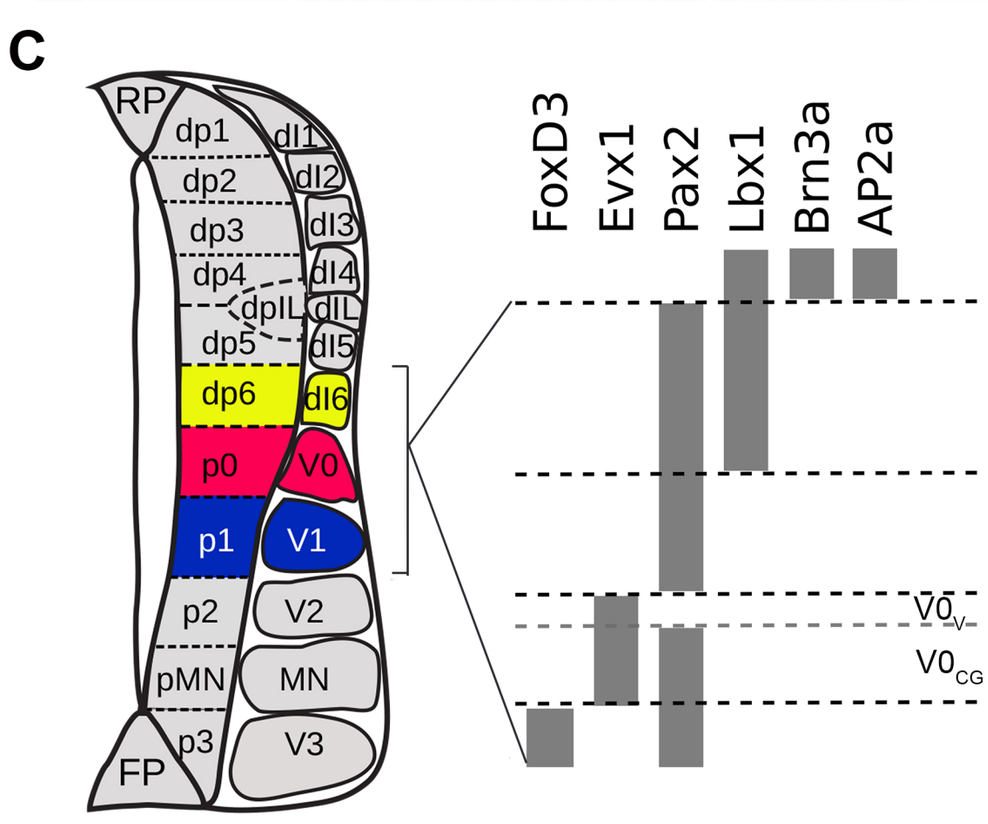

Gard et al., Figure 1

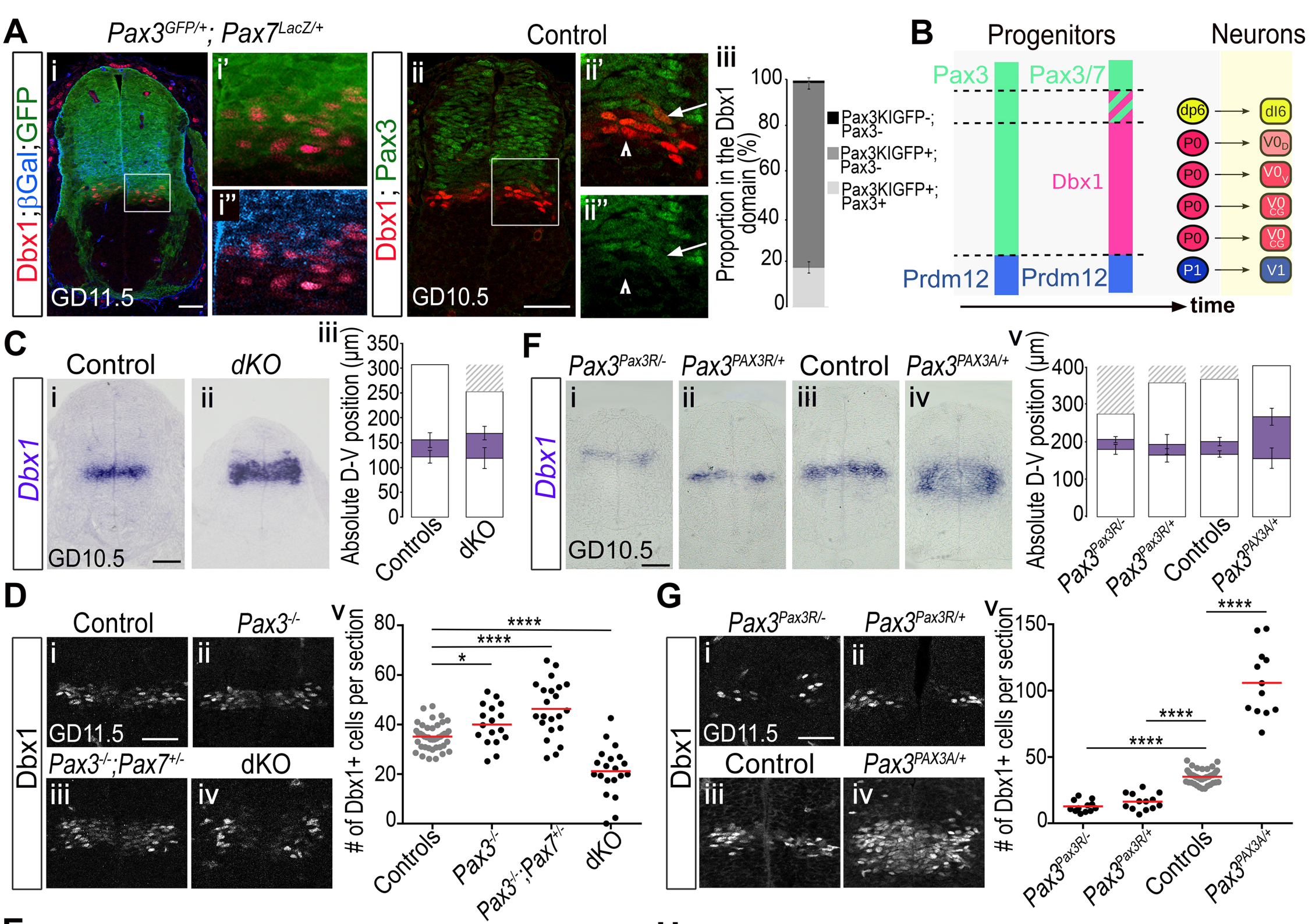

Gard et al., Figure 2

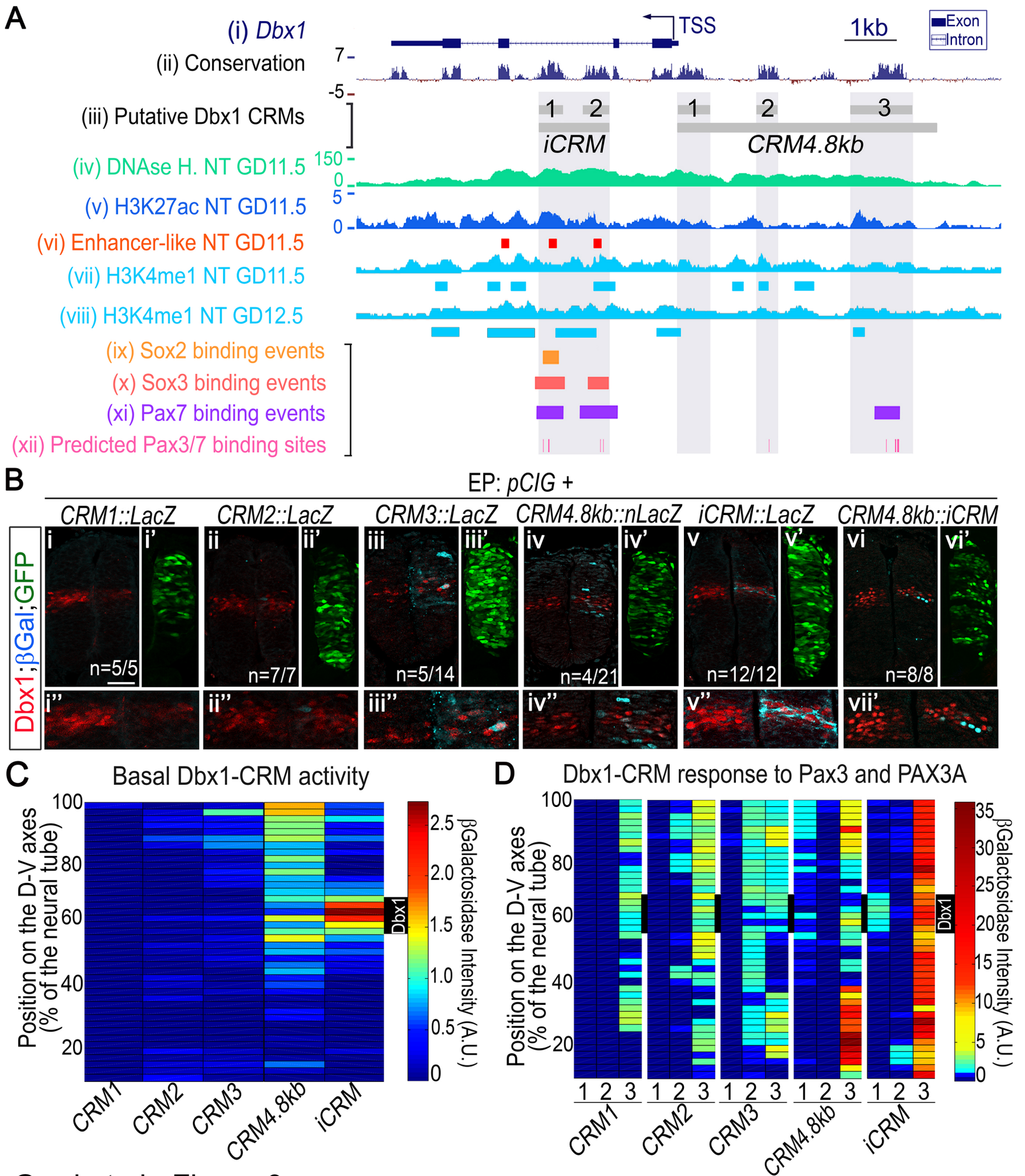
A
(i) Dbx1
(ii) Conservation
(iii) Putative Dbx1 CRMs
(iv) DNAse H. NT GD11.5
(v) H3K27ac NT GD11.5
(vi) Enhancer-like NT GD11.5
(vii) H3K4me1 NT GD11.5
(viii) H3K4me1 NT GD12.5
(ix) Sox2 binding events
(x) Sox3 binding events
(xi) Pax7 binding events
(xii) Predicted Pax3/7 binding sites
TSS
1kb
Exon
Intron
iCRM
CRM4.8kb
B
EP: pCIG +
CRM1::LacZ
CRM2::LacZ
CRM3::LacZ
CRM4.8kb::nLacZ
iCRM::LacZ
CRM4.8kb::iCRM
Dbx1;βGal;GFP
n=5/5
n=7/7
n=5/14
n=4/21
n=12/12
n=8/8
C
Basal Dbx1-CRM activity
Position on the D-V axes (% of the neural tube)
Dbx1
βGalactosidase Intensity (A.U.)
CRM1
CRM2
CRM3
CRM4.8kb
iCRM
D
Dbx1-CRM response to Pax3 and PAX3A
Gard et al., Figure 3

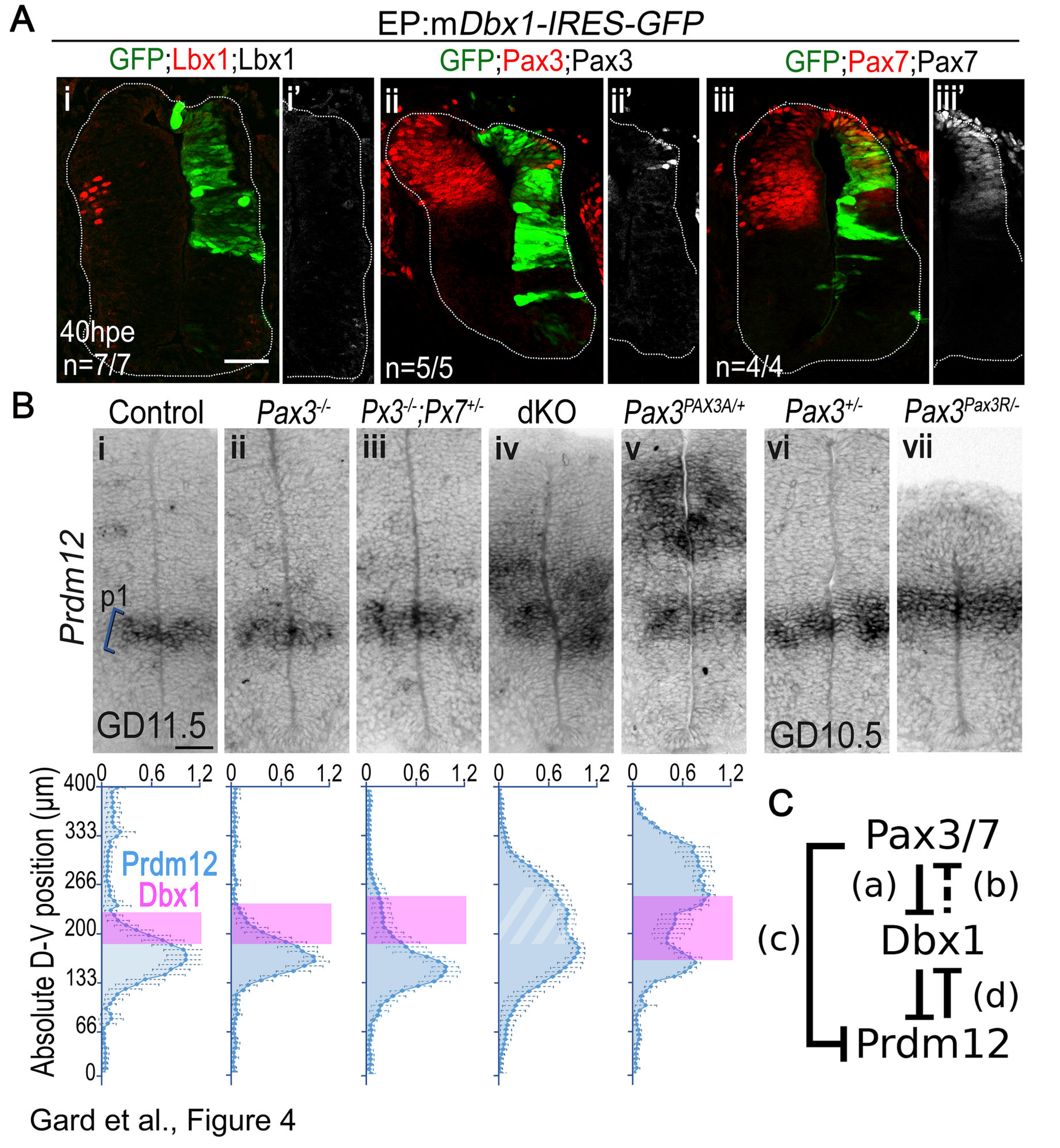

Gard et al., Figure 4

SUPPLEMENTARY MATERIAL

Pax3- and Pax7-mediated Dbx1 regulation orchestrates the patterning of intermediate spinal interneurons

Chris GARD[1*], Gloria GONZALEZ-CURTO[1*], Youcef El-Mokhtar FRARMA[1], Elodie CHOLLET[1], Nathalie DUVAL[1,2], Valentine AUZIÉ[1], Frédéric AURADÉ[3,4], Lisa VIGIER[1], Frédéric RELAIX[4], Alessandra PIERANI[1], Frédéric CAUSERET[1#] & Vanessa RIBES[1#]

[1] Institut Jacques Monod, CNRS UMR7592, Université Paris Diderot, Sorbonne Paris Cité, 75205 Paris Cedex, France

[2] Institut Pasteur, Department of developmental and stem cell biology, CNRS URA 2578, 75015 Paris, France

[3] Sorbonne Universités UPMC Univ Paris 06, Inserm, CNRS, Centre de Recherche en Myologie (CRM), GH Pitié Salpêtrière, 47 bld de l'hôpital, 75013 Paris, France

[4] INSERM IMRB U955-E10, UPEC - Université Paris Est, Faculté de Médicine, Créteil 94000, France

Supplementary Material and Methods

Electroporation constructs

Pax3 and Pax7 variants in pCIG vector and Dbx1 in pCAGGS vector

Pax3R and *Pax7R* were blunt subcloned into a *pCIG* EcoRV site from intermediate plasmids that were respectively cut by EcoRI or XhoI/SpeI. Pax3 was inserted into a *pCIG* EcoRI site from a plasmid kindly donated by P. Gruss. Pax7 was taken from the pPax7cp plasmid (gift from M.A. Rudnicki) using XhoI and MfeI restriction enzymes and inserted between XhoI and EcoRI sites in *pCIG*. The PAX3A construct was previously described (Relaix et al., 2003), while PAX7A was amplified by PCR from cDNA provided by F. Barr and cloned into XhoI and XmaI *pCIG* sites. We used a *pCAGG-IRES-EGFP* plasmid containing an HA tagged version of the mouse *Dbx1* gene (Karaz et al., 2016).

Reporter constructs for Dbx1 CRM activity

To generate the 4.8kbCRM reporter plasmid, a 4.8kb BamHI/BstEII fragment corresponding to sequences located immediately 5' to the Dbx1 TSS (Pierani et al., 2001) was inserted upstream of an *NLS-LacZ* cassette in a *pBluescript* vector. Sequences corresponding to CRM1, and CRM2 were individually amplified using the 4.8kbCRM construct as a template and the following primers:

CRM1-Fwd: AAAGCGGCCGCATCTGCTCTACGAGTCCCAT

CRM1-Rev: AAAACTAGTTACTTGGGCGTCTGCGAGT

CRM2-Fwd: AAAGCGGCCGCCCCTAAATAACTTTTTAATTTGA

CRM2-Rev: AAAACTAGTGCTCTGAGCCTCCACTGC

The iCRM sequence was amplified by PCR from mouse genomic DNA using the primers:

iCRM-Fwd: AAAGCGGCCGCTCCCTACCCCGAAGTCGTAT

iCRM-Rev: AAAACTAGTTCGTTTTAAAAACTACATATG

PCR products were subsequently cloned into the BGZA vector using NotI/SpeI restriction sites in order to match with the CRM3 reporter plasmid (Oosterveen et al., 2012). For the 4.8kbCRM+iCRM construct, the sequence corresponding to the iCRM was inserted into the 4.8kbCRM reporter plasmid after the *LacZ* cassette, in order to mimic the genomic context.

Dbx1 mutant mouse line

The knock-in mouse line carrying *LacZ* in the *Dbx1* locus was previously described (Pierani et al., 2001).

Immunohistochemistry and *in situ* hybridisation

The following primary antibodies were used: rabbit anti-Dbx1 (Pierani et al., 1999), chick anti-GFP (1/1000, Abcam), mouse anti-β-Galactosidase (1/500, Promega), mouse anti-Evx1 (1/500, DSHB), mouse anti-Pax3 (1/100, DSHB), mouse anti-Pax7 (1/100, DSHB), mouse anti-Brn3a (1/500, gift from C. Parras), guinea-pig anti-FoxD3 (1/10,000, gift from T. Muller/C. Birchmeier), rabbit and guinea-pig anti-Lbx1 (1/10,000, gift from T. Muller/C. Birchmeier), rabbit anti-AP2α (1/500, Santa-Cruz), goat anti-Lhx2 (1:250, Santa Cruz), rabbit anti-Pax2 (1/500, Thermo Scientific), goat anti-Sox9 (1/500, R&D). Secondary antibodies were all from Thermo Scientific, coupled to Alexa Fluorophores (A488, A568, A647) and diluted 1/500. Immunofluorescence microscopy was carried out using a Leica TCS SP5 confocal microscope. For *in situ* hybridisation experiments, we used probes against mouse *Dbx1* (Lu et al., 1994), chick *Dbx1* (Pierani et al., 1999) and mouse *Prmd12* (Kinameri et al., 2008). Pictures were then taken with an Axio Observer Z1 microscope (Zeiss). All the images were processed with Photoshop 7.0 software (Adobe Systems, San Jose, CA, USA) or Image J v.1.43 g image analysis software (NIH).

Defining Pax3 and Pax7 specific position weight matrices

Position weight matrices (PWMs) for Pax homeodomain binding sites were taken from work by (Jolma et al., 2013) or created *de novo* from Pax3 and Pax7 ChIP-Sequencing data (Soleimani et al., 2012) using MEME (Supp. Fig. 3A). Pax3 and Pax7 peak location data were retrieved for the top 500 ChIP peaks and 100bp sequences either side of their centre were fetched using Galaxy (usegalaxy.org). A Pax7 HD PWM was created using 200bp sequences of the top 500 peaks using MEME. The PWM for the Pax3 paired domain binding site was created by selecting 51 sequences from the ChIP-Seq data that contained at least three consecutive bases of the core GTCAC motif. These sequences were reduced to 100 base pairs in length and used in MEME to establish the PWM.

Defining the transcription factors expressed in GD11.5 mouse neural tube

Genes with an expression level below 0 TPM in the ENCODE RNAseq screen performed on GD11.5 mouse spinal cord (ENCODE project, accession number: ENCSR337FYI) were annotated with gene ontology terms using the Bioconductor packages AnnotationDbi (Pagès H, Carlson M, Falcon S and Li N (2017). *AnnotationDbi: Annotation Database Interface*. R package version 1.36.2.) and Mus.musculus (Team BC (2015). *Mus.musculus: Annotation package for the Mus.musculus object*. R package version 1.3.1.). Genes annotated under the GO term "sequence-specific DNA binding" were selected (Supp. Table 4).

Supplementary Table 1. **Number of embryos and sections used for quantifications of cell number per sections at GD11.5**

Pax3$^{-/-}$		*Pax3*$^{-/-}$; *Pax7*$^{+/-}$		*dKO*		*Control*		*Pax3*$^{Pax3R/-}$		*Pax3*$^{Pax3R/+}$		*Pax3*$^{PAX3A/+}$	
Number of dI6 cells per section at GD11.5 - cf Graphs Fig. 1Bi,v													
4	*10*	**9**	*21*	**3**	*8*	**13**	*23*	**1**	*3*	**2**	*5*	**3**	*9*
Number of V0$_D$ cells per section at GD11.5 - cf Graphs Fig. 1Bii, vi													
2	*9*	**6**	*11*	nd	nd	**7**	*15*	nd	nd	**4**	*7*	**4**	*8*
Number of V0$_{VCG}$ cells per section at GD11.5 - cf Graphs Fig. 1Biii, vii													
7	*15*	**14**	*35*	**8**	*21*	**31**	*73*	**11**	*24*	**5**	*10*	**18**	*45*
Number of V1 cells per section at GD11.5 - cf Graphs Fig. 1Biv, viii													
7	*14*	**15**	*36*	**9**	*21*	**27**	*68*	**8**	*23*	**7**	*13*	**12**	*35*
Number of Dbx1$^+$ cells per section at GD11.5 - cf Graphs Fig. 2Dv, Gv													
5	*16*	**7**	*21*	**5**	*19*	**17**	*43*	**4**	*11*	**5**	*12*	**6**	*11*

In **bold** are given the numbers of embryos analysed

In *Italics* are given the numbers of sections considered

Supplementary Table 2. **Number of embryos and sections used for generating the heatmaps in Fig. 3C and 3D**

CRM1 + pCIG		*CRM1 + Pax3*		*CRM1 + PAX3A*		*CRM2 + pCIG*		*CRM2 + Pax3*		*CRM2 + PAX3A*	
5	*5*	**5**	*5*	**3**	*4*	**7**	*7*	**5**	*7*	**5**	*7*
CRM3 + pCIG		*CRM3 + Pax3*		*CRM3 + PAX3A*		*CRM4.8kb + pCIG*		*CRM4.8kb + Pax3*		*CRM4.8kb + PAX3A*	
7	*7*	**5**	*5*	**5**	*5*	**10**	*17*	**4**	*6*	**6**	*6*
iCRM + pCIG		*iCRM + Pax3*		*iCRM + PAX3A*							
9	*9*	**5**	*8*	**6**	*9*						

In **bold** are given the numbers of embryos analysed

In *Italics* are given the numbers of sections considered

Supplementary Table 3. Mann–Whitney *U* test probabilities.

All comparisons are done to control embryos.

***Pax3*$^{-/-}$**	***Pax3*$^{-/-}$; *Pax7*$^{+/-}$**	***dKO***		***Pax3*$^{Pax3R/-}$**	***Pax3*$^{Pax3R/+}$**	***Pax3*$^{PAX3A/+}$**
Number of dI6 cells per section at GD11.5 - cf Graphs Fig. 1Bi,v						
0.0167	< 0.0001	< 0.0001		0.3446	0.0992	< 0.0001
Number of $V0_D$ cells per section at GD11.5 - cf Graphs Fig. 1Bii, vi						
0.0024	0.0002	NA		NA	0.0233	< 0.0001
Number of $V0_{VCG}$ cells per section at GD11.5 - cf Graphs Fig. 1Biii, vii						
< 0.0001	< 0.0001	< 0.0001		< 0.0001	0.0009	< 0.0001
Number of V1 cells per section at GD11.5 - cf Graphs Fig. 1Biv, viii						
< 0.0001	< 0.0001	< 0.0001		0.2658	0.3328	0.0072
Number of $Dbx1^+$ cells per section at GD11.5 - cf Graphs Fig. 2Dv, Gv						
0.0223	< 0.0001	< 0.0001		< 0.0001	< 0.0001	< 0.0001

Significant differences are highlighted in orange

Supplementary Table 4. Transcription factors expressed in GD11.5 mouse spinal cord.

ENSEMBLE gene ID	MGI SYMBOL	Expression (TPM)	ENSEMBLE gene ID	MGI SYMBOL	Expression (TPM)	ENSEMBLE gene ID	MGI SYMBOL	Expression (TPM)	ENSEMBLE gene ID	MGI SYMBOL	Expression (TPM)
ENSMUSG00000000078	Klf6	24.39	ENSMUSG00000022463	Srebf2	103.48	ENSMUSG00000032238	Rora	2.55	ENSMUSG00000048280	Zfp738	11.27
ENSMUSG00000000093	Tbx2	3.17	ENSMUSG00000022479	Vdr	0.13	ENSMUSG00000032292	Nr2e3	0.06	ENSMUSG00000048349	Pou4f1	76.1
ENSMUSG00000000094	Tbx4	0.19	ENSMUSG00000022484	Hoxc10	47.89	ENSMUSG00000032318	Isl2	42.04	ENSMUSG00000048377	Foxi2	0.07
ENSMUSG00000000134	Tfe3	20.25	ENSMUSG00000022485	Hoxc5	29.18	ENSMUSG00000032368	Zic1	14.22	ENSMUSG00000048402	Gli2	9.5
ENSMUSG00000000247	Lhx2	6.91	ENSMUSG00000022508	Bcl6	0.13	ENSMUSG00000032376	Usp3	81.54	ENSMUSG00000048450	Msx1	43.75
ENSMUSG00000000266	Mid2	5.14	ENSMUSG00000022510	Trp63	4.34	ENSMUSG00000032398	Snapc5	42.25	ENSMUSG00000048481	Mypop	4.15
ENSMUSG00000000275	Trim25	1.91	ENSMUSG00000022521	Crebbp	28.31	ENSMUSG00000032402	Smad3	12.05	ENSMUSG00000048482	Bdnf	2.31
ENSMUSG00000000282	Mnt	5.45	ENSMUSG00000022526	Zfp251	29.18	ENSMUSG00000032411	Tfdp2	50.68	ENSMUSG00000048490	Nrip1	28.98
ENSMUSG00000000317	Bcl6b	4.95	ENSMUSG00000022528	Hes1	45.03	ENSMUSG00000032419	Tbx18	2.3	ENSMUSG00000048528	Nkx1-2	1.02
ENSMUSG00000000435	Myf5	9.27	ENSMUSG00000022529	Zfp263	21.2	ENSMUSG00000032481	Smarcc1	79.39	ENSMUSG00000048540	Nhlh2	67.01
ENSMUSG00000000440	Pparg	0.13	ENSMUSG00000022556	Hsf1	46.82	ENSMUSG00000032501	Trib1	17.17	ENSMUSG00000048581	E130311K13Rik	2.49
ENSMUSG00000000567	Sox9	127.4	ENSMUSG00000022676	Snai2	20.41	ENSMUSG00000032515	Csrnp1	0.66	ENSMUSG00000048728	Zfp454	12.61
ENSMUSG00000000690	Hoxb6	69.42	ENSMUSG00000022682	Rrn3	96.57	ENSMUSG00000032652	Crebl2	1.16	ENSMUSG00000048756	Foxo3	3.08
ENSMUSG00000000708	Kat2b	4.11	ENSMUSG00000022683	Pla2g10	0.06	ENSMUSG00000032691	Nlrp3	0.08	ENSMUSG00000048763	Hoxb3	8
ENSMUSG00000000731	Aire	0.1	ENSMUSG00000022710	Usp7	30.76	ENSMUSG00000032698	Lmo2	21.9	ENSMUSG00000048776	Pthlh	1.22
ENSMUSG00000000782	Tcf7	10.08	ENSMUSG00000022811	Zfp148	32.26	ENSMUSG00000032744	Heyl	26.8	ENSMUSG00000048904	Neurog1	35.39
ENSMUSG00000000861	Bcl11a	57.5	ENSMUSG00000022828	Gtf2e1	43.84	ENSMUSG00000032745	Gpbp1	105.63	ENSMUSG00000049086	Bmyc	54.08
ENSMUSG00000000869	Il4	3.15	ENSMUSG00000022838	Eaf2	0.97	ENSMUSG00000032815	Fanca	18.31	ENSMUSG00000049164	Zfp518a	11.56
ENSMUSG00000000902	Smarcb1	233.16	ENSMUSG00000022895	Ets2	18.05	ENSMUSG00000032897	Nfyc	99.8	ENSMUSG00000049295	Zfp219	53.62
ENSMUSG00000000938	Hoxa10	57.75	ENSMUSG00000022952	Runx1	0.93	ENSMUSG00000032998	Foxj3	16.94	ENSMUSG00000049321	Zfp2	27.33
ENSMUSG00000000942	Hoxa4	9.26	ENSMUSG00000022974	Paxbp1	66.12	ENSMUSG00000033006	Sox10	26.04	ENSMUSG00000049421	Zfp260	107.77
ENSMUSG00000001156	Mxd1	17.7	ENSMUSG00000022987	Zfp641	1.53	ENSMUSG00000033016	Nfatc1	2.15	ENSMUSG00000049532	Sall2	43.18
ENSMUSG00000001228	Uhrf1	101.85	ENSMUSG00000022996	Wnt10b	0.6	ENSMUSG00000033080	Vsx1	0.78	ENSMUSG00000049577	Zfpm1	1.12
ENSMUSG00000001280	Sp1	9.38	ENSMUSG00000022997	Wnt1	10.22	ENSMUSG00000033249	Hsf4	0.07	ENSMUSG00000049604	Hoxb13	0.26
ENSMUSG00000001288	Rarg	19.02	ENSMUSG00000023027	Atf1	19.45	ENSMUSG00000033276	Stk36	17.91	ENSMUSG00000049672	Zbtb14	23.48
ENSMUSG00000001418	Glmp	54.87	ENSMUSG00000023034	Nr4a1	3.52	ENSMUSG00000033542	Arhgef5	2.05	ENSMUSG00000049691	Nkx3-2	1.96
ENSMUSG00000001419	Mef2d	14.26	ENSMUSG00000023055	Calcoco1	31.95	ENSMUSG00000033543	Gtf2a2	154.14	ENSMUSG00000049728	Zfp668	21.1
ENSMUSG00000001444	Tbx21	0.16	ENSMUSG00000023079	Gtf2ird1	39.21	ENSMUSG00000033585	Ndn	372.16	ENSMUSG00000049791	Fzd4	3.57
ENSMUSG00000001472	Tcf25	133.57	ENSMUSG00000023110	Prmt5	97.94	ENSMUSG00000033669	Zfp7	9.91	ENSMUSG00000050100	Hmx2	1.39
ENSMUSG00000001493	Meox1	15.8	ENSMUSG00000023391	Dlx2	1.77	ENSMUSG00000033713	Foxn3	69.8	ENSMUSG00000050288	Fzd2	29.57
ENSMUSG00000001497	Pax9	2.92	ENSMUSG00000023411	Nfatc4	15.24	ENSMUSG00000033726	Emx1	0.05	ENSMUSG00000050295	Foxc1	8.7
ENSMUSG00000001504	Irx2	17.73	ENSMUSG00000023826	Park2	0.86	ENSMUSG00000033740	St18	25.57	ENSMUSG00000050328	Hoxc12	3.65
ENSMUSG00000001510	Dlx3	1.75	ENSMUSG00000023882	Zfp54	3.49	ENSMUSG00000033837	Foxh1	0.65	ENSMUSG00000050368	Hoxd10	23.23
ENSMUSG00000001517	Foxm1	43.12	ENSMUSG00000023892	Zfp51	13.39	ENSMUSG00000033863	Klf9	0.99	ENSMUSG00000050397	Foxl2	0.15
ENSMUSG00000001524	Gtf2h4	33.98	ENSMUSG00000023902	Zscan10	0.06	ENSMUSG00000033871	Ppargc1b	1.1	ENSMUSG00000050619	Zscan29	11.83
ENSMUSG00000001552	Jup	38.22	ENSMUSG00000023927	Satb1	26.44	ENSMUSG00000033883	D3Ertd254e	8.32	ENSMUSG00000050747	Trim15	0.33
ENSMUSG00000001566	Mnx1	6.02	ENSMUSG00000023990	Tfeb	1.44	ENSMUSG00000033943	Mga	28.43	ENSMUSG00000050846	Zfp623	25.47
ENSMUSG00000001627	Ifrd1	128.89	ENSMUSG00000023991	Foxp4	27.39	ENSMUSG00000033961	Zfp446	6.14	ENSMUSG00000050855	Zfp940	9.83
ENSMUSG00000001655	Hoxc13	3.58	ENSMUSG00000023994	Nfya	21.92	ENSMUSG00000034023	Fancd2	10.67	ENSMUSG00000050945	Zfp438	2.72
ENSMUSG00000001656	Hoxc11	1.62	ENSMUSG00000024014	Pim1	11.6	ENSMUSG00000034041	Lyl1	3.64	ENSMUSG00000051034	Zfp11	6.47

ENSMUSG00000001657	Hoxc8	50.52	ENSMUSG00000024081	Cebpz	23.49	ENSMUSG00000034042	Gpbp1l1	24.96	ENSMUSG00000051159	Cited1	4.74
ENSMUSG00000001661	Hoxc6	75.86	ENSMUSG00000024134	Six2	1.21	ENSMUSG00000034057	Myrfl	0.37	ENSMUSG00000051251	Nhlh1	10.95
ENSMUSG00000001729	Akt1	99.79	ENSMUSG00000024137	E4f1	10.45	ENSMUSG00000034071	Zfp551	4.09	ENSMUSG00000051316	Taf7	18.47
ENSMUSG00000001815	Evx2	0.54	ENSMUSG00000024140	Epas1	6.93	ENSMUSG00000034161	Scx	9.62	ENSMUSG00000051341	Zfp52	1.29
ENSMUSG00000001819	Hoxd13	0.79	ENSMUSG00000024176	Sox8	7.5	ENSMUSG00000034227	Foxj1	2.45	ENSMUSG00000051351	Zfp46	27.06
ENSMUSG00000001823	Hoxd12	1.62	ENSMUSG00000024206	Rfx2	3.29	ENSMUSG00000034266	Batf	1.04	ENSMUSG00000051367	Six1	27.79
ENSMUSG00000001911	Nfix	2.93	ENSMUSG00000024215	Spdef	0.08	ENSMUSG00000034271	Jdp2	0.51	ENSMUSG00000051413	Plagl2	26.99
ENSMUSG00000001988	Npas1	0.34	ENSMUSG00000024238	Zeb1	29.88	ENSMUSG00000034341	Wbp2	83.07	ENSMUSG00000051451	Crebzf	28.63
ENSMUSG00000002028	Kmt2a	8.5	ENSMUSG00000024276	Zfp397	31.63	ENSMUSG00000034384	Barhl2	3.09	ENSMUSG00000051469	Zfp24	80.43
ENSMUSG00000002057	Foxn1	0.02	ENSMUSG00000024401	Tnf	0.12	ENSMUSG00000034429	Zfp707	14.87	ENSMUSG00000051510	Mafg	21.6
ENSMUSG00000002108	Nr1h3	0.88	ENSMUSG00000024431	Nr3c1	5.34	ENSMUSG00000034430	Zxdc	7.68	ENSMUSG00000051675	Trim32	60.96
ENSMUSG00000002111	Spi1	2.22	ENSMUSG00000024454	Hdac3	108	ENSMUSG00000034460	Six4	6.74	ENSMUSG00000051817	Sox12	15.14
ENSMUSG00000002147	Stat6	5.43	ENSMUSG00000024457	Trim26	29.8	ENSMUSG00000034486	Gbx2	36.53	ENSMUSG00000051910	Sox6	15.34
ENSMUSG00000002249	Tead3	3.49	ENSMUSG00000024497	Pou4f3	2.61	ENSMUSG00000034522	Zfp395	11.14	ENSMUSG00000051977	Prdm9	0.79
ENSMUSG00000002250	Ppard	1.7	ENSMUSG00000024498	Tcerg1	59.66	ENSMUSG00000034538	Zfp418	3.01	ENSMUSG00000052040	Klf13	26.74
ENSMUSG00000002266	Zim1	1.8	ENSMUSG00000024513	Mbd2	11.68	ENSMUSG00000034673	Pbx2	13.76	ENSMUSG00000052056	Zfp217	2.6
ENSMUSG00000002325	Irf9	4.68	ENSMUSG00000024515	Smad4	35.84	ENSMUSG00000034701	Neurod1	35.54	ENSMUSG00000052135	Foxo6	0.35
ENSMUSG00000002345	Mef2b	41.38	ENSMUSG00000024560	Cxxc1	30.39	ENSMUSG00000034762	Glis1	1.84	ENSMUSG00000052271	Bhlha15	0.07
ENSMUSG00000002393	Nr2f6	66.45	ENSMUSG00000024563	Smad2	52.99	ENSMUSG00000034777	Vax2	0.1	ENSMUSG00000052435	Cebpe	0.05
ENSMUSG00000002428	Hltf	17.79	ENSMUSG00000024565	Sall3	15.51	ENSMUSG00000034800	Zfp661	7.8	ENSMUSG00000052534	Pbx1	36.29
ENSMUSG00000002578	Ikzf4	3.94	ENSMUSG00000024619	Cdx1	0.2	ENSMUSG00000034957	Cebpa	0.15	ENSMUSG00000052684	Jun	39.32
ENSMUSG00000002617	Zfp40	15.27	ENSMUSG00000024777	Ppp2r5b	47.93	ENSMUSG00000035011	Zbtb7a	6.93	ENSMUSG00000052837	Junb	4.83
ENSMUSG00000002983	Relb	2.96	ENSMUSG00000024789	Jak2	11.31	ENSMUSG00000035033	Tbr1	0.23	ENSMUSG00000052942	Glis3	1.26
ENSMUSG00000003032	Klf4	1.06	ENSMUSG00000024826	Dpf2	162.14	ENSMUSG00000035041	Creb3l3	0.56	ENSMUSG00000053007	Creb5	3.18
ENSMUSG00000003051	Elf3	1.11	ENSMUSG00000024837	Dmrt1	0.12	ENSMUSG00000035125	Gcfc2	9.63	ENSMUSG00000053110	Yap1	21.48
ENSMUSG00000003154	Foxj2	4.04	ENSMUSG00000024912	Fosl1	0.24	ENSMUSG00000035158	Mitf	1.06	ENSMUSG00000053129	Gsx1	8.92
ENSMUSG00000003184	Irf3	45.75	ENSMUSG00000024913	Lrp5	2.99	ENSMUSG00000035187	Nkx6-1	4.62	ENSMUSG00000053175	Bcl3	0.86
ENSMUSG00000003282	Plag1	1.99	ENSMUSG00000024922	Ovol1	0.26	ENSMUSG00000035277	Arx	1.37	ENSMUSG00000053178	Mterf1b	2.91
ENSMUSG00000003283	Hck	1.34	ENSMUSG00000024927	Rela	24.71	ENSMUSG00000035397	Klf16	4.37	ENSMUSG00000053470	Kdm3a	38.87
ENSMUSG00000003308	Keap1	25.51	ENSMUSG00000024947	Men1	53.39	ENSMUSG00000035451	Foxa1	1.3	ENSMUSG00000053477	Tcf4	98.59
ENSMUSG00000003382	Etv3	6.84	ENSMUSG00000024955	Esrra	2.85	ENSMUSG00000035478	Mbd3	215.2	ENSMUSG00000053552	Ebf4	1.62
ENSMUSG00000003423	Pih1d1	85.3	ENSMUSG00000024968	Rcor2	27.83	ENSMUSG00000035576	L3mbtl1	0.05	ENSMUSG00000053747	Sox14	3.33
ENSMUSG00000003662	Ciao1	56.12	ENSMUSG00000024985	Tcf7l2	47.14	ENSMUSG00000035799	Twist1	16.67	ENSMUSG00000053985	Zfp14	5.07
ENSMUSG00000003847	Nfat5	6.94	ENSMUSG00000024986	Hhex	3.51	ENSMUSG00000035868	3110052M02Rik	9.18	ENSMUSG00000054160	Nkx2-4	0.03
ENSMUSG00000003868	Ruvbl2	116.45	ENSMUSG00000025019	Lcor	22.49	ENSMUSG00000035877	Zhx3	8.41	ENSMUSG00000054191	Klf1	10.17
ENSMUSG00000003923	Tfam	62.63	ENSMUSG00000025034	Trim8	24.86	ENSMUSG00000035923	Myf6	2.28	ENSMUSG00000054321	Taf4b	1.39
ENSMUSG00000003949	Hlf	0.73	ENSMUSG00000025049	Taf5	8.18	ENSMUSG00000035934	Pknox2	17.94	ENSMUSG00000054381	Zfp747	6.38
ENSMUSG00000004040	Stat3	34.44	ENSMUSG00000025050	Pcgf6	22.85	ENSMUSG00000035946	Gsx2	5.06	ENSMUSG00000054604	Cggbp1	99.58
ENSMUSG00000004043	Stat5a	1.02	ENSMUSG00000025056	Nr0b1	0.2	ENSMUSG00000036098	Myrf	1.39	ENSMUSG00000054648	Zfp869	29.37
ENSMUSG00000004151	Etv1	10.98	ENSMUSG00000025128	Bhlhe22	1.42	ENSMUSG00000036139	Hoxc9	28.63	ENSMUSG00000054715	Zscan22	15.54
ENSMUSG00000004231	Pax2	6.36	ENSMUSG00000025172	Ankrd2	0.33	ENSMUSG00000036144	Meox2	8.65	ENSMUSG00000054717	Hmgb2	316.93
ENSMUSG00000004264	Phb2	293.52	ENSMUSG00000025215	Tlx1	0.23	ENSMUSG00000036180	Gatad2a	55.26	ENSMUSG00000054737	Zfp182	5.88
ENSMUSG00000004328	Hif3a	5.92	ENSMUSG00000025216	Lbx1	6.14	ENSMUSG00000036192	Rorb	1.99	ENSMUSG00000054808	Actn4	145.03
ENSMUSG00000004359	Spic	0.1	ENSMUSG00000025223	Ldb1	75.41	ENSMUSG00000036461	Elf1	6.85	ENSMUSG00000054892	Txk	0.05
ENSMUSG00000004661	Arid3b	20.49	ENSMUSG00000025225	Nfkb2	3.04	ENSMUSG00000036602	Alx1	0.7	ENSMUSG00000054931	Zkscan4	3.2
ENSMUSG00000004842	Pou1f1	0.03	ENSMUSG00000025229	Pitx3	1.74	ENSMUSG00000036686	Cc2d1a	8.93	ENSMUSG00000054939	Zfp174	0.84
ENSMUSG00000004872	Pax3	33.97	ENSMUSG00000025255	Zfhx4	33.74	ENSMUSG00000036721	Zscan12	18	ENSMUSG00000054967	Zfp647	21.26

ENSMUSG00000004897	Hdgf	202.43	ENSMUSG00000025323	Sp4	12.92	ENSMUSG00000036867	Smad6	5.41	ENSMUSG00000055024	Ep300	16.16
ENSMUSG00000005148	Klf5	2.61	ENSMUSG00000025364	Pa2g4	219.16	ENSMUSG00000036923	Stox1	0.89	ENSMUSG00000055053	Nfic	12.84
ENSMUSG00000005267	Zfp287	11.39	ENSMUSG00000025369	Smarcc2	85.36	ENSMUSG00000036940	Kdm1a	80.63	ENSMUSG00000055067	Smyd3	15.59
ENSMUSG00000005373	Mlxipl	0.43	ENSMUSG00000025373	Rnf41	22.19	ENSMUSG00000036972	Zic4	45.71	ENSMUSG00000055116	Arntl	6.26
ENSMUSG00000005413	Hmox1	12.38	ENSMUSG00000025407	Gli1	2.86	ENSMUSG00000036980	Taf6	99	ENSMUSG00000055148	Klf2	4.78
ENSMUSG00000005503	Evx1	1.48	ENSMUSG00000025408	Ddit3	17.29	ENSMUSG00000037001	Zfp39	5.73	ENSMUSG00000055210	Foxd2	0.42
ENSMUSG00000005533	Igf1r	12.65	ENSMUSG00000025423	Pias2	64.9	ENSMUSG00000037007	Zfp113	19.75	ENSMUSG00000055228	Zfp935	11.61
ENSMUSG00000005566	Trim28	419.76	ENSMUSG00000025469	Msx3	81.49	ENSMUSG00000037017	Zscan21	102.03	ENSMUSG00000055313	Pgbd1	3.91
ENSMUSG00000005583	Mef2c	14.09	ENSMUSG00000025494	Sigirr	1.33	ENSMUSG00000037025	Foxa2	3.2	ENSMUSG00000055320	Tead1	10.23
ENSMUSG00000005672	Kit	17.71	ENSMUSG00000025498	Irf7	0.69	ENSMUSG00000037029	Zfp146	11.63	ENSMUSG00000055341	Zfp457	0.14
ENSMUSG00000005677	Nr1i3	0.05	ENSMUSG00000025529	Zfp711	21.6	ENSMUSG00000037034	Pax1	13.48	ENSMUSG00000055435	Maf	4.34
ENSMUSG00000005698	Ctcf	85.05	ENSMUSG00000025602	Zfp202	5.49	ENSMUSG00000037138	Aff3	22.77	ENSMUSG00000055491	Pprc1	36.01
ENSMUSG00000005718	Tfap4	13.58	ENSMUSG00000025612	Bach1	18.01	ENSMUSG00000037169	Mycn	84.65	ENSMUSG00000055639	Dach1	17.27
ENSMUSG00000005774	Rfx5	5.61	ENSMUSG00000025782	Taf3	13.31	ENSMUSG00000037171	Nodal	0.03	ENSMUSG00000055799	Tcf7l1	17.28
ENSMUSG00000005836	Gata6	0.45	ENSMUSG00000025880	Smad7	3.73	ENSMUSG00000037174	Elf2	36.64	ENSMUSG00000055817	Mta3	29.62
ENSMUSG00000005886	Ncoa2	23.93	ENSMUSG00000025902	Sox17	8.46	ENSMUSG00000037188	Grhl3	3.33	ENSMUSG00000055835	Zfp1	16.66
ENSMUSG00000005893	Nr2c2	15.7	ENSMUSG00000025912	Mybl1	3.65	ENSMUSG00000037214	Thap1	17.3	ENSMUSG00000055917	Zfp277	32.78
ENSMUSG00000005897	Nr2c1	9.46	ENSMUSG00000025927	Tfap2b	38.23	ENSMUSG00000037279	Ovol2	0.04	ENSMUSG00000055991	Zkscan5	16.7
ENSMUSG00000005917	Otx1	0.17	ENSMUSG00000025930	Msc	6.26	ENSMUSG00000037335	Hand1	0.43	ENSMUSG00000056216	Cebpg	28.85
ENSMUSG00000006215	Zbtb17	38.39	ENSMUSG00000025958	Creb1	48.57	ENSMUSG00000037343	Taf2	28.59	ENSMUSG00000056493	Foxk1	2.47
ENSMUSG00000006311	Etv2	0.06	ENSMUSG00000025959	Klf7	27.29	ENSMUSG00000037369	Kdm6a	21.29	ENSMUSG00000056501	Cebpb	2.38
ENSMUSG00000006362	Cbfa2t3	7.49	ENSMUSG00000025997	Ikzf2	2.66	ENSMUSG00000037373	Ctbp1	377.15	ENSMUSG00000056537	Rlim	36.78
ENSMUSG00000006498	Ptbp1	169.24	ENSMUSG00000026017	Carf	4.29	ENSMUSG00000037465	Klf10	23.24	ENSMUSG00000056648	Hoxb8	22.18
ENSMUSG00000006586	Runx1t1	37.06	ENSMUSG00000026021	Sumo1	398.52	ENSMUSG00000037523	Mavs	12.08	ENSMUSG00000056749	Nfil3	24.08
ENSMUSG00000006705	Pknox1	36.71	ENSMUSG00000026077	Npas2	0.13	ENSMUSG00000037601	Nme1	202.68	ENSMUSG00000056758	Hmga2	39.39
ENSMUSG00000006720	Zfp184	17.46	ENSMUSG00000026104	Stat1	12.31	ENSMUSG00000037621	Atoh8	5.83	ENSMUSG00000056820	Tsnax	119.82
ENSMUSG00000006932	Ctnnb1	536.21	ENSMUSG00000026234	Ncl	288.57	ENSMUSG00000037640	Zfp60	66.23	ENSMUSG00000056829	Foxb2	0.08
ENSMUSG00000007216	Zfp775	6.42	ENSMUSG00000026313	Hdac4	25.46	ENSMUSG00000037674	Rfx7	17.82	ENSMUSG00000056854	Pou3f4	6.26
ENSMUSG00000007415	Gatad1	57.96	ENSMUSG00000026321	Tnfrsf11a	0.57	ENSMUSG00000037791	Phf12	15.74	ENSMUSG00000057093	C030039L03Rik	3.91
ENSMUSG00000007805	Twist2	12.68	ENSMUSG00000026374	Tsn	295.18	ENSMUSG00000037868	Egr2	0.58	ENSMUSG00000057098	Ebf1	88.51
ENSMUSG00000007812	Zfp655	33.12	ENSMUSG00000026380	Tfcp2l1	0.07	ENSMUSG00000037894	H2afz	1953.87	ENSMUSG00000057156	Homez	16.92
ENSMUSG00000007872	Id3	348.73	ENSMUSG00000026398	Nr5a2	0.44	ENSMUSG00000037935	Smarce1	152.19	ENSMUSG00000057173	Rfx8	0.12
ENSMUSG00000007946	Phox2a	1.48	ENSMUSG00000026436	Elk4	14.72	ENSMUSG00000037984	Neurod6	0.92	ENSMUSG00000057236	Rbbp4	380.44
ENSMUSG00000008398	Elk3	14.1	ENSMUSG00000026459	Myog	38.23	ENSMUSG00000037992	Rara	57.96	ENSMUSG00000057406	Whsc1	87.66
ENSMUSG00000008496	Pou2f2	32.04	ENSMUSG00000026468	Lhx4	10.84	ENSMUSG00000038151	Prdm1	1.15	ENSMUSG00000057409	Zfp53	8.59
ENSMUSG00000008575	Nfib	22.98	ENSMUSG00000026484	Rnf2	120.35	ENSMUSG00000038193	Hand2	0.17	ENSMUSG00000057469	E2f6	50.65
ENSMUSG00000008855	Hdac5	34.55	ENSMUSG00000026491	Ahctf1	28.39	ENSMUSG00000038203	Hoxa13	0.08	ENSMUSG00000057522	Spop	100.85
ENSMUSG00000008976	Gabpa	33.78	ENSMUSG00000026497	Mixl1	0.08	ENSMUSG00000038210	Hoxa11	4.8	ENSMUSG00000057551	Zfp317	22.74
ENSMUSG00000009097	Tbx1	3.05	ENSMUSG00000026536	Mnda	0.4	ENSMUSG00000038227	Hoxa9	79.32	ENSMUSG00000057691	Zfp746	15.71
ENSMUSG00000009248	Ascl2	0.37	ENSMUSG00000026565	Pou2f1	21.84	ENSMUSG00000038236	Hoxa7	55.62	ENSMUSG00000057842	Zfp595	1.4
ENSMUSG00000009406	Elk1	5.45	ENSMUSG00000026586	Prrx1	24.24	ENSMUSG00000038253	Hoxa5	42.33	ENSMUSG00000057895	Zfp105	29.07
ENSMUSG00000009471	Myod1	7.94	ENSMUSG00000026610	Esrrg	10.06	ENSMUSG00000038255	Neurod2	0.93	ENSMUSG00000057982	Zfp809	6.27
ENSMUSG00000009555	Cdk9	67.12	ENSMUSG00000026628	Atf3	2.51	ENSMUSG00000038331	Satb2	1.19	ENSMUSG00000058099	Nfam1	2.38
ENSMUSG00000009569	Mkl2	17.86	ENSMUSG00000026630	Batf3	3.77	ENSMUSG00000038342	Mlxip	17.46	ENSMUSG00000058192	Zfp846	12.1
ENSMUSG00000009733	Tfcp2	16.21	ENSMUSG00000026637	Traf5	4.01	ENSMUSG00000038346	Zfp384	7.59	ENSMUSG00000058230	Arhgap35	45.18
ENSMUSG00000009734	Pou6f2	1.8	ENSMUSG00000026638	Irf6	4.37	ENSMUSG00000038402	Foxf2	4.11	ENSMUSG00000058239	Usf2	23.11
ENSMUSG00000009739	Pou6f1	6.83	ENSMUSG00000026641	Usf1	127.86	ENSMUSG00000038415	Foxq1	2.43	ENSMUSG00000058291	Zfp68	63.47

ENSMUSG00000009741	Ubp1	36.15	ENSMUSG00000026646	Suv39h2	32.21	ENSMUSG00000038418	Egr1	2.44	ENSMUSG00000058318	Phf21a	27
ENSMUSG00000009900	Wnt3a	2.64	ENSMUSG00000026663	Atf6	9.45	ENSMUSG00000038482	Tfdp1	153.66	ENSMUSG00000058331	Zfp85	4.45
ENSMUSG00000010175	Prox1	10.96	ENSMUSG00000026674	Ddr2	28.05	ENSMUSG00000038518	Jarid2	37.9	ENSMUSG00000058402	Zfp420	9.23
ENSMUSG00000010476	Ebf3	8.54	ENSMUSG00000026686	Lmx1a	2.92	ENSMUSG00000038533	Cbfa2t2	50.03	ENSMUSG00000058440	Nrf1	60.91
ENSMUSG00000010505	Myt1	29.98	ENSMUSG00000026700	Tnfsf4	0.03	ENSMUSG00000038539	Atf5	2.04	ENSMUSG00000058638	Zfp110	23.4
ENSMUSG00000010797	Wnt2	2.64	ENSMUSG00000026735	Ptf1a	10.79	ENSMUSG00000038550	Ciart	2.65	ENSMUSG00000058665	En1	4.15
ENSMUSG00000012350	Ehf	0.11	ENSMUSG00000026739	Bmi1	34.63	ENSMUSG00000038615	Nfe2l1	36.3	ENSMUSG00000058669	Nkx2-9	0.67
ENSMUSG00000012396	Nanog	0.06	ENSMUSG00000026751	Nr5a1	0.06	ENSMUSG00000038630	Zkscan16	1.05	ENSMUSG00000058756	Thra	25.36
ENSMUSG00000012520	Phox2b	1.21	ENSMUSG00000026805	Barhl1	7.4	ENSMUSG00000038648	Creb3l2	11.44	ENSMUSG00000058794	Nfe2	5.13
ENSMUSG00000013089	Etv5	15.51	ENSMUSG00000026826	Nr4a2	4.8	ENSMUSG00000038679	Trps1	17.4	ENSMUSG00000058881	Zfp516	10.08
ENSMUSG00000013663	Pten	6.45	ENSMUSG00000026843	Fubp3	68.74	ENSMUSG00000038692	Hoxb4	3.03	ENSMUSG00000058883	Zfp708	4.34
ENSMUSG00000013787	Ehmt2	50.09	ENSMUSG00000026890	Lhx6	0.57	ENSMUSG00000038700	Hoxb5	38.94	ENSMUSG00000058886	Deaf1	45.89
ENSMUSG00000014030	Pax5	1.87	ENSMUSG00000026923	Notch1	47.94	ENSMUSG00000038705	Gmeb2	16.99	ENSMUSG00000058900	Rsl1	3.46
ENSMUSG00000014039	Prdm15	10.47	ENSMUSG00000026932	Nacc2	7.62	ENSMUSG00000038718	Pbx3	69.66	ENSMUSG00000059213	Ddn	0.38
ENSMUSG00000014303	Glis2	28.68	ENSMUSG00000026934	Lhx3	20.08	ENSMUSG00000038721	Hoxb7	52.22	ENSMUSG00000059246	Foxb1	2.94
ENSMUSG00000014592	Camta1	59.85	ENSMUSG00000026942	Traf2	23.28	ENSMUSG00000038765	Lmx1b	1.31	ENSMUSG00000059291	Rpl11	316.52
ENSMUSG00000014603	Alx3	0.47	ENSMUSG00000026976	Pax8	20.6	ENSMUSG00000038797	Zscan2	3.45	ENSMUSG00000059436	Max	14.77
ENSMUSG00000014704	Hoxa2	30.64	ENSMUSG00000027102	Hoxd8	18.27	ENSMUSG00000038805	Six3	0.11	ENSMUSG00000059552	Trp53	133.82
ENSMUSG00000014767	Tbp	66.37	ENSMUSG00000027104	Atf2	65.37	ENSMUSG00000038845	Phb	178.78	ENSMUSG00000059669	Taf1b	25.01
ENSMUSG00000014859	E2f4	80.34	ENSMUSG00000027109	Sp3	53.47	ENSMUSG00000038872	Zfhx3	29.02	ENSMUSG00000059824	Dbp	2.77
ENSMUSG00000015053	Gata2	4.7	ENSMUSG00000027164	Traf6	17.41	ENSMUSG00000038909	Kat7	70.05	ENSMUSG00000059897	Zfp930	14.06
ENSMUSG00000015092	Edf1	271.47	ENSMUSG00000027168	Pax6	22.32	ENSMUSG00000039005	Tlr4	0.66	ENSMUSG00000060314	Zfp941	6.14
ENSMUSG00000015120	Ube2i	612.01	ENSMUSG00000027186	Elf5	0.1	ENSMUSG00000039086	Ss18l1	16.58	ENSMUSG00000060336	Zfp937	11.11
ENSMUSG00000015461	Atf6b	70.02	ENSMUSG00000027210	Meis2	93.02	ENSMUSG00000039087	Rreb1	4.69	ENSMUSG00000060373	Hnrnpc	347.7
ENSMUSG00000015501	Hivep2	5.78	ENSMUSG00000027230	Creb3l1	1.56	ENSMUSG00000039095	En2	0.02	ENSMUSG00000060397	Zfp128	5.51
ENSMUSG00000015522	Arnt	21.46	ENSMUSG00000027387	Zc3h8	7.23	ENSMUSG00000039117	Taf4	6.11	ENSMUSG00000060477	Irak2	1.32
ENSMUSG00000015579	Nkx2-5	0.04	ENSMUSG00000027433	Xrn2	86.87	ENSMUSG00000039153	Runx2	1.06	ENSMUSG00000060601	Nr1h2	55.15
ENSMUSG00000015605	Srf	3.51	ENSMUSG00000027434	Nkx2-2	5.25	ENSMUSG00000039158	Akna	4.72	ENSMUSG00000060743	H3f3a	2565.29
ENSMUSG00000015619	Gata3	6.85	ENSMUSG00000027439	Gzf1	21.61	ENSMUSG00000039191	Rbpj	45.34	ENSMUSG00000060969	Irx1	1.49
ENSMUSG00000015627	Gata5	0.12	ENSMUSG00000027490	E2f1	11.03	ENSMUSG00000039231	Suv39h1	67.15	ENSMUSG00000061013	Mkx	5.22
ENSMUSG00000015709	Arnt2	20.88	ENSMUSG00000027544	Nfatc2	0.74	ENSMUSG00000039238	Zfp750	0.46	ENSMUSG00000061311	Rag1	0.13
ENSMUSG00000015839	Nfe2l2	21.01	ENSMUSG00000027547	Sall4	6.15	ENSMUSG00000039275	Foxk2	16.32	ENSMUSG00000061360	Phf5a	176.84
ENSMUSG00000015843	Rxrg	6.57	ENSMUSG00000027552	E2f5	54.32	ENSMUSG00000039377	Hlx	7.42	ENSMUSG00000061371	Zfp873	9.47
ENSMUSG00000015846	Rxra	5.71	ENSMUSG00000027582	Zgpat	36.51	ENSMUSG00000039410	Prdm16	8.5	ENSMUSG00000061436	Hipk2	24.16
ENSMUSG00000015937	H2afy	485.52	ENSMUSG00000027660	Skil	47.65	ENSMUSG00000039474	Wfs1	7.07	ENSMUSG00000061517	Sox21	10.14
ENSMUSG00000016087	Fli1	18	ENSMUSG00000027667	Zfp639	38.55	ENSMUSG00000039476	Prrx2	7.13	ENSMUSG00000061524	Zic2	4.97
ENSMUSG00000016458	Wt1	1.04	ENSMUSG00000027671	Actl6a	185.1	ENSMUSG00000039477	Tnrc18	21.12	ENSMUSG00000061544	Zfp229	5.81
ENSMUSG00000016477	E2f3	13.6	ENSMUSG00000027678	Ncoa3	17.73	ENSMUSG00000039521	Foxp3	0.04	ENSMUSG00000061894	Zscan20	3.54
ENSMUSG00000016503	Gtf3a	69.73	ENSMUSG00000027684	Mecom	25.2	ENSMUSG00000039634	Zfp189	11.93	ENSMUSG00000061911	Myt1l	4.89
ENSMUSG00000016559	H3f3b	1424.99	ENSMUSG00000027794	Sohlh2	0.07	ENSMUSG00000039656	Rxrb	20.31	ENSMUSG00000062012	Zfp13	15.86
ENSMUSG00000016624	Phf21b	25.47	ENSMUSG00000027796	Smad9	0.45	ENSMUSG00000039671	Zmynd8	42.03	ENSMUSG00000062040	Zfp27	11.46
ENSMUSG00000017007	Rbpjl	0.01	ENSMUSG00000027833	Shox2	16.5	ENSMUSG00000039699	Batf2	0.15	ENSMUSG00000062115	Rai1	22.27
ENSMUSG00000017491	Rarb	57.44	ENSMUSG00000027859	Ngf	0.7	ENSMUSG00000039741	Bahcc1	15.58	ENSMUSG00000062116	Zfp954	14.6
ENSMUSG00000017548	Suz12	16.9	ENSMUSG00000027868	Tbx15	1.7	ENSMUSG00000039830	Olig2	1.67	ENSMUSG00000062327	T	1.66
ENSMUSG00000017667	Zfp334	18.25	ENSMUSG00000027938	Creb3l4	2.74	ENSMUSG00000039834	Zfp335	11.03	ENSMUSG00000062329	Cytl1	1.02
ENSMUSG00000017688	Hnf4g	0.08	ENSMUSG00000027967	Neurog2	32.66	ENSMUSG00000039852	Rere	40.36	ENSMUSG00000062563	Cys1	1.23
ENSMUSG00000017724	Etv4	7.41	ENSMUSG00000027985	Lef1	20.37	ENSMUSG00000039853	Trim14	0.71	ENSMUSG00000062713	Sim2	0.14

ENSMUSG00000017801	Mlx	47.87	ENSMUSG00000028023	Pitx2	12.77	ENSMUSG00000039910	Cited2	64.29	ENSMUSG00000062743	Zfp677	3.03
ENSMUSG00000017861	Mybl2	21.54	ENSMUSG00000028042	Zbtb7b	0.2	ENSMUSG00000039997	Ifi203	0.39	ENSMUSG00000062794	Zfp599	5.1
ENSMUSG00000017950	Hnf4a	0.01	ENSMUSG00000028086	Fbxw7	18.16	ENSMUSG00000040007	Bahd1	1.15	ENSMUSG00000062861	Zfp28	7.51
ENSMUSG00000018143	Mafk	6.56	ENSMUSG00000028161	Ppp3ca	55.52	ENSMUSG00000040033	Stat2	10.9	ENSMUSG00000062939	Stat4	0.86
ENSMUSG00000018160	Med1	58.93	ENSMUSG00000028163	Nfkb1	12.23	ENSMUSG00000040054	Baz2a	12.43	ENSMUSG00000062944	9130023H24Rik	10.19
ENSMUSG00000018168	Ikzf3	0.07	ENSMUSG00000028266	Lmo4	52.05	ENSMUSG00000040123	Zmym5	13.64	ENSMUSG00000063047	Zfp780b	3.34
ENSMUSG00000018263	Tbx5	0.36	ENSMUSG00000028341	Nr4a3	0.43	ENSMUSG00000040138	Ndp	6.12	ENSMUSG00000063060	Sox7	7.63
ENSMUSG00000018347	Zkscan6	11.52	ENSMUSG00000028417	Tal2	0.16	ENSMUSG00000040148	Hmx3	1.11	ENSMUSG00000063065	Mapk3	42.69
ENSMUSG00000018476	Kdm6b	33.3	ENSMUSG00000028423	Nfx1	72.44	ENSMUSG00000040167	Ikzf5	26.66	ENSMUSG00000063108	Zfp26	24.18
ENSMUSG00000018501	Ncor1	138.66	ENSMUSG00000028466	Creb3	49.77	ENSMUSG00000040187	Arntl2	0.83	ENSMUSG00000063281	Zfp35	25.53
ENSMUSG00000018548	Trim37	62.32	ENSMUSG00000028517	Plpp3	38.3	ENSMUSG00000040209	Zfp704	4.98	ENSMUSG00000063358	Mapk1	170.96
ENSMUSG00000018604	Tbx3	7.59	ENSMUSG00000028565	Nfia	22.69	ENSMUSG00000040270	Bach2	23.49	ENSMUSG00000063535	Zfp773	5.31
ENSMUSG00000018651	Tada2a	25.98	ENSMUSG00000028582	Cc2d1b	13.99	ENSMUSG00000040289	Hey1	38.85	ENSMUSG00000063632	Sox11	476.41
ENSMUSG00000018654	Ikzf1	2.52	ENSMUSG00000028610	Dmrtb1	4.57	ENSMUSG00000040310	Alx4	1.67	ENSMUSG00000063659	Zbtb18	9.04
ENSMUSG00000018678	Sp2	23.52	ENSMUSG00000028634	Hivep3	3.93	ENSMUSG00000040321	Zfp770	4.29	ENSMUSG00000063672	Nkx6-3	0.1
ENSMUSG00000018697	Aatf	43.67	ENSMUSG00000028639	Ybx1	1001.84	ENSMUSG00000040390	Map3k10	7.01	ENSMUSG00000063870	Chd4	98.25
ENSMUSG00000018698	Lhx1	36.7	ENSMUSG00000028640	Tfap2c	1.02	ENSMUSG00000040433	Zbtb38	9.97	ENSMUSG00000063889	Crem	14.21
ENSMUSG00000018750	Zbtb4	0.79	ENSMUSG00000028654	Mycl	80.26	ENSMUSG00000040463	Mybbp1a	116.89	ENSMUSG00000063894	Zkscan8	8.18
ENSMUSG00000018822	Sfrp5	3.28	ENSMUSG00000028707	Dmbx1	0.61	ENSMUSG00000040481	Bptf	33.22	ENSMUSG00000063972	Nr6a1	4.95
ENSMUSG00000018899	Irf1	3.14	ENSMUSG00000028717	Tal1	5.87	ENSMUSG00000040489	Sox30	0.08	ENSMUSG00000066224	Arid3c	0.94
ENSMUSG00000018973	Hoxb1	13.59	ENSMUSG00000028736	Pax7	3	ENSMUSG00000040610	Tlx3	22.57	ENSMUSG00000066456	Hmgn3	82.36
ENSMUSG00000018983	E2f2	5.7	ENSMUSG00000028756	Pink1	23.16	ENSMUSG00000040629	Mael	0.04	ENSMUSG00000066613	Zfp932	18.32
ENSMUSG00000019230	Lhx9	8.9	ENSMUSG00000028800	Hdac1	204.51	ENSMUSG00000040712	Camta2	8.43	ENSMUSG00000066687	Zbtb16	3.82
ENSMUSG00000019256	Ahr	3.86	ENSMUSG00000028820	Sfpq	124.38	ENSMUSG00000040726	Hesx1	0.05	ENSMUSG00000066838	Zfp772	8.79
ENSMUSG00000019564	Arid3a	5.3	ENSMUSG00000028890	Mtf1	12.11	ENSMUSG00000040732	Erg	1.66	ENSMUSG00000066839	Ecsit	30.31
ENSMUSG00000019768	Esr1	0.06	ENSMUSG00000028899	Taf12	46.53	ENSMUSG00000040761	Spen	12.98	ENSMUSG00000067071	Hes6	250.56
ENSMUSG00000019777	Hdac2	355.16	ENSMUSG00000028901	Gmeb1	32.61	ENSMUSG00000040841	Six5	5.86	ENSMUSG00000067261	Foxd3	4.41
ENSMUSG00000019789	Hey2	3.57	ENSMUSG00000028964	Park7	330.24	ENSMUSG00000040857	Erf	13.08	ENSMUSG00000067438	Hmx1	6.85
ENSMUSG00000019803	Nr2e1	0.08	ENSMUSG00000028975	Pex14	34.08	ENSMUSG00000040891	Foxa3	0.03	ENSMUSG00000067724	Gbx1	1.01
ENSMUSG00000019817	Plagl1	118.59	ENSMUSG00000028988	Ctnnbip1	52.18	ENSMUSG00000040929	Rfx3	22.48	ENSMUSG00000067860	Zic3	15.41
ENSMUSG00000019826	Zbtb24	13.96	ENSMUSG00000029003	Mad2l2	57.07	ENSMUSG00000041000	Trim62	16.33	ENSMUSG00000067931	Zfp948	16.27
ENSMUSG00000019878	Hsf2	42.52	ENSMUSG00000029026	Trp73	0.24	ENSMUSG00000041168	Lonp1	43.98	ENSMUSG00000067942	Zfp160	11.45
ENSMUSG00000019900	Rfx6	0.12	ENSMUSG00000029075	Tnfrsf4	0.36	ENSMUSG00000041187	Prkd2	8.03	ENSMUSG00000068130	Zfp442	7.17
ENSMUSG00000019913	Sim1	1.54	ENSMUSG00000029127	Zbtb49	15.77	ENSMUSG00000041235	Chd7	89.29	ENSMUSG00000068154	Insm1	7.33
ENSMUSG00000019947	Arid5b	10.51	ENSMUSG00000029135	Fosl2	0.43	ENSMUSG00000041309	Nkx6-2	5.61	ENSMUSG00000068327	Tlx2	23.94
ENSMUSG00000019982	Myb	3.51	ENSMUSG00000029167	Ppargc1a	2.4	ENSMUSG00000041343	Ankrd42	7.7	ENSMUSG00000068457	Uty	8.34
ENSMUSG00000020037	Rfx4	49.77	ENSMUSG00000029191	Rfc1	59.92	ENSMUSG00000041420	Meis3	153.05	ENSMUSG00000068551	Zfp467	8.96
ENSMUSG00000020038	Cry1	27.19	ENSMUSG00000029196	Tada2b	3.3	ENSMUSG00000041483	Zfp281	32.16	ENSMUSG00000068742	Cry2	16.94
ENSMUSG00000020052	Ascl1	32.09	ENSMUSG00000029238	Clock	5.94	ENSMUSG00000041515	Irf8	2.79	ENSMUSG00000068959	Zfp619	3.16
ENSMUSG00000020063	Sirt1	10.55	ENSMUSG00000029249	Rest	19.85	ENSMUSG00000041530	Ago1	20.81	ENSMUSG00000069171	Nr2f1	46.38
ENSMUSG00000020086	H2afy2	194.68	ENSMUSG00000029313	Aff1	8.68	ENSMUSG00000041540	Sox5	24.48	ENSMUSG00000069184	Zfp72	4.99
ENSMUSG00000020160	Meis1	150.77	ENSMUSG00000029475	Kdm2b	59.29	ENSMUSG00000041565	L3mbtl4	0.18	ENSMUSG00000069727	Gm5595	7.63
ENSMUSG00000020167	Tcf3	141.82	ENSMUSG00000029478	Ncor2	19.22	ENSMUSG00000041703	Zic5	8.13	ENSMUSG00000070345	Hsf5	0.19
ENSMUSG00000020185	E2f7	23.39	ENSMUSG00000029484	Anxa3	23.28	ENSMUSG00000041730	Prrxl1	12.01	ENSMUSG00000070420	Zscan25	0.35
ENSMUSG00000020230	Prmt2	91	ENSMUSG00000029546	Uncx	41.48	ENSMUSG00000041852	Tcf20	8.17	ENSMUSG00000070493	Chchd2	802.88
ENSMUSG00000020232	Hmg20b	82.34	ENSMUSG00000029556	Hnf1a	0.02	ENSMUSG00000041911	Dlx1	0.93	ENSMUSG00000070495	Ctcfl	0.04
ENSMUSG00000020248	Nfyb	58.36	ENSMUSG00000029563	Foxp2	24.46	ENSMUSG00000042002	Foxn4	1.34	ENSMUSG00000070544	Top1	82.94

ENSMUSG00000020275	Rel	0.74	ENSMUSG00000029580	Actb	5603.4	ENSMUSG00000042063	Zfp386	56.05	ENSMUSG00000070632	Btbd8	2.17
ENSMUSG00000020335	Zfp354b	1.29	ENSMUSG00000029587	Zfp12	21.85	ENSMUSG00000042197	Zfp451	37.28	ENSMUSG00000070643	Sox13	9.73
ENSMUSG00000020358	Hnrnpab	602.52	ENSMUSG00000029595	Lhx5	24.35	ENSMUSG00000042258	Isl1	109.32	ENSMUSG00000070691	Runx3	2.38
ENSMUSG00000020364	Zfp354a	6.76	ENSMUSG00000029627	Zkscan14	6.74	ENSMUSG00000042292	Mkl1	18.62	ENSMUSG00000070709	1700049G17Rik	10.56
ENSMUSG00000020420	Zfp607	2.2	ENSMUSG00000029687	Ezh2	95.94	ENSMUSG00000042372	Dmrt3	1.87	ENSMUSG00000070822	Zscan18	7.33
ENSMUSG00000020453	Patz1	83.04	ENSMUSG00000029705	Cux1	86.03	ENSMUSG00000042390	Gatad2b	6.94	ENSMUSG00000071054	Safb	91.88
ENSMUSG00000020472	Zkscan17	20.57	ENSMUSG00000029723	Tsc22d4	57.86	ENSMUSG00000042406	Atf4	105.31	ENSMUSG00000071076	Jund	62.12
ENSMUSG00000020473	Aebp1	7.13	ENSMUSG00000029729	Zkscan1	35.28	ENSMUSG00000042448	Hoxd1	7.74	ENSMUSG00000071256	Zfp213	18.73
ENSMUSG00000020484	Xbp1	131.03	ENSMUSG00000029754	Dlx6	0.03	ENSMUSG00000042477	Tfap2e	0.08	ENSMUSG00000071291	Zfp58	14.03
ENSMUSG00000020538	Srebf1	42.29	ENSMUSG00000029755	Dlx5	0.59	ENSMUSG00000042499	Hoxd11	6.74	ENSMUSG00000071646	Mta2	45.55
ENSMUSG00000020542	Myocd	1.98	ENSMUSG00000029771	Irf5	1.78	ENSMUSG00000042557	Sin3a	43.8	ENSMUSG00000071665	Foxr2	0.11
ENSMUSG00000020601	Trib2	62.72	ENSMUSG00000029832	Nfe2l3	0.34	ENSMUSG00000042589	Cux2	10.52	ENSMUSG00000071757	Zhx2	6.49
ENSMUSG00000020644	Id2	234.2	ENSMUSG00000029833	Trim24	31.64	ENSMUSG00000042596	Tfap2d	0.17	ENSMUSG00000072294	Klf12	15.41
ENSMUSG00000020653	Klf11	13.07	ENSMUSG00000029836	Cbx3	487.86	ENSMUSG00000042622	Maff	0.98	ENSMUSG00000072889	Nfxl1	20.6
ENSMUSG00000020656	Grhl1	0.48	ENSMUSG00000029840	Mtpn	120.48	ENSMUSG00000042745	Id1	92.13	ENSMUSG00000073043	Atoh1	13.61
ENSMUSG00000020679	Hnf1b	0.22	ENSMUSG00000029844	Hoxa1	7.36	ENSMUSG00000042750	Bex2	236.45	ENSMUSG00000073176	Zfp449	6.51
ENSMUSG00000020871	Dlx4	0.09	ENSMUSG00000029913	Prdm5	10.56	ENSMUSG00000042812	Foxf1	2.07	ENSMUSG00000073489	Ifi204	0.45
ENSMUSG00000020875	Hoxb9	54.04	ENSMUSG00000030001	Figla	0.08	ENSMUSG00000042821	Snai1	25.58	ENSMUSG00000073490	AI607873	0.44
ENSMUSG00000020888	Dvl2	30.83	ENSMUSG00000030067	Foxp1	91.7	ENSMUSG00000042895	Abra	0.03	ENSMUSG00000074151	Nlrc5	0.03
ENSMUSG00000020889	Nr1d1	1.54	ENSMUSG00000030087	Klf15	2.23	ENSMUSG00000042903	Foxo4	2.11	ENSMUSG00000074158	9830147E19Rik	1.1
ENSMUSG00000020893	Per1	8.39	ENSMUSG00000030103	Bhlhe40	2.77	ENSMUSG00000043013	Onecut1	6.73	ENSMUSG00000074220	Zfp382	8.76
ENSMUSG00000020914	Top2a	268.02	ENSMUSG00000030189	Ybx3	43.07	ENSMUSG00000043099	Hic1	3.26	ENSMUSG00000074221	Zfp568	12.85
ENSMUSG00000020919	Stat5b	14.44	ENSMUSG00000030199	Etv6	13.31	ENSMUSG00000043219	Hoxa6	12.65	ENSMUSG00000074406	Zfp628	3.03
ENSMUSG00000020923	Ubtf	74.19	ENSMUSG00000030201	Lrp6	14.67	ENSMUSG00000043263	Pyhin1	0.02	ENSMUSG00000074519	Etohi1	11.12
ENSMUSG00000020950	Foxg1	0.69	ENSMUSG00000030232	Aebp2	10.15	ENSMUSG00000043342	Hoxd9	11.29	ENSMUSG00000074622	Mafb	10.53
ENSMUSG00000020954	Strn3	38.3	ENSMUSG00000030256	Bhlhe41	0.83	ENSMUSG00000043456	Zfp536	18.1	ENSMUSG00000074637	Sox2	26.22
ENSMUSG00000021010	Npas3	10.09	ENSMUSG00000030353	Tead4	1.55	ENSMUSG00000043535	Setx	9.77	ENSMUSG00000074676	Foxs1	0.37
ENSMUSG00000021055	Esr2	0.09	ENSMUSG00000030380	Mzf1	1.75	ENSMUSG00000043602	Zfp3	8.38	ENSMUSG00000074731	Zfp345	0.02
ENSMUSG00000021067	Sav1	8.84	ENSMUSG00000030386	Zfp606	38.21	ENSMUSG00000043753	Dmrta1	0.29	ENSMUSG00000074824	Rslcan18	0.23
ENSMUSG00000021095	Gsc	0.43	ENSMUSG00000030393	Zik1	37.77	ENSMUSG00000043866	Taf10	152.03	ENSMUSG00000074865	Zfp934	10.12
ENSMUSG00000021098	4930447C04Rik	1.48	ENSMUSG00000030424	Zfp939	4.02	ENSMUSG00000043909	Trp53bp1	116.78	ENSMUSG00000074867	Zfp808	7.51
ENSMUSG00000021109	Hif1a	103.48	ENSMUSG00000030443	Zfp583	6.49	ENSMUSG00000043962	Thrap3	155.51	ENSMUSG00000075304	Sp5	1.81
ENSMUSG00000021144	Mta1	17.03	ENSMUSG00000030446	Zfp273	5.36	ENSMUSG00000043969	Emx2	1.32	ENSMUSG00000075394	Hoxc4	53.38
ENSMUSG00000021156	Zmynd11	80.68	ENSMUSG00000030469	Zfp719	14.58	ENSMUSG00000043991	Pura	1.56	ENSMUSG00000075588	Hoxb2	70.44
ENSMUSG00000021239	Vsx2	5.89	ENSMUSG00000030470	Csrp3	1.95	ENSMUSG00000044167	Foxo1	3.37	ENSMUSG00000076431	Sox4	128.34
ENSMUSG00000021250	Fos	1.99	ENSMUSG00000030507	Dbx1	14.71	ENSMUSG00000044220	Nkx2-3	0.08	ENSMUSG00000078302	Foxd1	8.77
ENSMUSG00000021255	Esrrb	0.75	ENSMUSG00000030543	Mesp2	0.61	ENSMUSG00000044296	Zfp879	0.44	ENSMUSG00000078427	Sarnp	142.22
ENSMUSG00000021264	Yy1	18.89	ENSMUSG00000030551	Nr2f2	49.8	ENSMUSG00000044312	Neurog3	10.01	ENSMUSG00000078496	Gm13152	4.87
ENSMUSG00000021318	Gli3	25.34	ENSMUSG00000030557	Mef2a	22.99	ENSMUSG00000044501	Zfp758	7.04	ENSMUSG00000078502	Gm13212	1.28
ENSMUSG00000021319	Sfrp4	1.28	ENSMUSG00000030604	Zfp626	0.93	ENSMUSG00000044518	Foxe3	0.15	ENSMUSG00000078580	E430018J23Rik	5.55
ENSMUSG00000021326	Trim27	92.64	ENSMUSG00000030678	Maz	66.8	ENSMUSG00000044636	Csrnp2	24.31	ENSMUSG00000078619	Smarcd2	35.28
ENSMUSG00000021327	Zkscan3	57.88	ENSMUSG00000030699	Tbx6	0.31	ENSMUSG00000044646	Zbtb7c	2.17	ENSMUSG00000078671	Chd2	15.89
ENSMUSG00000021356	Irf4	0.01	ENSMUSG00000030757	Zkscan2	5.15	ENSMUSG00000044647	Csrnp3	12.99	ENSMUSG00000078779	Zfp59	9.26
ENSMUSG00000021359	Tfap2a	9.29	ENSMUSG00000030793	Pycard	2.94	ENSMUSG00000044674	Fzd1	15	ENSMUSG00000078866	Gm14420	7.92
ENSMUSG00000021362	Gcm2	0.06	ENSMUSG00000030796	Tead2	205.03	ENSMUSG00000044676	Zfp612	9.51	ENSMUSG00000078896	Gm14436	5.37
ENSMUSG00000021366	Hivep1	8.41	ENSMUSG00000030823	9130019O22Rik	7.02	ENSMUSG00000044807	Zfp354c	38.67	ENSMUSG00000079033	Mef2b	0.46
ENSMUSG00000021381	Barx1	0.04	ENSMUSG00000030966	Trim21	0.1	ENSMUSG00000044876	Zfp444	55.99	ENSMUSG00000079037	Prnp	26.24

ENSMUSG00000021457	Syk	3.05	ENSMUSG00000031079	Zfp300	1.96	ENSMUSG00000044934	Zfp367	11.37	ENSMUSG00000079056	Kcnip3	2.67
ENSMUSG00000021466	Ptch1	15.38	ENSMUSG00000031103	Elf4	1.81	ENSMUSG00000045179	Sox3	8.7	ENSMUSG00000079215	Zfp664	123.24
ENSMUSG00000021469	Msx2	16.02	ENSMUSG00000031162	Gata1	3.89	ENSMUSG00000045268	Zfp691	9	ENSMUSG00000079277	Hoxd3	43.5
ENSMUSG00000021488	Nsd1	25.28	ENSMUSG00000031241	Tbx22	0.07	ENSMUSG00000045302	Preb	81.64	ENSMUSG00000079487	Med12	32.8
ENSMUSG00000021506	Pitx1	2.05	ENSMUSG00000031311	Nono	522.48	ENSMUSG00000045333	Zfp423	31.54	ENSMUSG00000079509	Zfx	19.23
ENSMUSG00000021514	Zfp369	7.96	ENSMUSG00000031323	Dmrtc1a	0.64	ENSMUSG00000045466	Zfp956	7.16	ENSMUSG00000079560	Hoxa3	16.02
ENSMUSG00000021540	Smad5	44.7	ENSMUSG00000031328	Flna	192.32	ENSMUSG00000045515	Pou3f3	9.01	ENSMUSG00000079681	Zglp1	0.92
ENSMUSG00000021546	Hnrnpk	2038.29	ENSMUSG00000031365	Zfp275	14.31	ENSMUSG00000045518	Onecut3	1	ENSMUSG00000087598	Zfp111	9.49
ENSMUSG00000021604	Irx4	1.73	ENSMUSG00000031393	Mecp2	11.64	ENSMUSG00000045519	Zfp560	24.68	ENSMUSG00000089756	Gm8898	3.33
ENSMUSG00000021685	Otp	6.38	ENSMUSG00000031431	Tsc22d3	121.11	ENSMUSG00000045639	Zfp629	29.92	ENSMUSG00000090125	Pou3f1	13.59
ENSMUSG00000021690	Jmy	2.86	ENSMUSG00000031451	Gas6	5.05	ENSMUSG00000045757	Zfp764	5.98	ENSMUSG00000090272	Mndal	0.38
ENSMUSG00000021775	Nr1d2	3.74	ENSMUSG00000031540	Kat6a	19.68	ENSMUSG00000045903	Npas4	0.09	ENSMUSG00000090641	Zfp712	4.12
ENSMUSG00000021779	Thrb	0.36	ENSMUSG00000031618	Nr3c2	0.92	ENSMUSG00000045991	Onecut2	6.39	ENSMUSG00000090659	Zfp493	2.19
ENSMUSG00000021796	Bmpr1a	40.53	ENSMUSG00000031627	Irf2	4.98	ENSMUSG00000046160	Olig1	0.38	ENSMUSG00000091183	Gm5141	8.71
ENSMUSG00000021848	Otx2	0.26	ENSMUSG00000031665	Sall1	27.99	ENSMUSG00000046179	E2f8	13.09	ENSMUSG00000091764	Zfp964	1.23
ENSMUSG00000021938	Pspc1	53.72	ENSMUSG00000031681	Smad1	55.43	ENSMUSG00000046351	Zfp322a	48.52	ENSMUSG00000092260	Zfp963	6.96
ENSMUSG00000021944	Gata4	0.49	ENSMUSG00000031688	Pou4f2	2.1	ENSMUSG00000046470	Sox18	14.32	ENSMUSG00000092416	Zfp141	9.07
ENSMUSG00000021994	Wnt5a	9.97	ENSMUSG00000031706	Rfx1	6.28	ENSMUSG00000046518	Ferd3l	0.57	ENSMUSG00000093668	Pou5f2	0.82
ENSMUSG00000022010	Tsc22d1	518.92	ENSMUSG00000031728	Zfp821	39.55	ENSMUSG00000046532	Ar	0.08	ENSMUSG00000094483	Purb	10.19
ENSMUSG00000022015	Tnfsf11	0.21	ENSMUSG00000031734	Irx3	13.31	ENSMUSG00000046572	Zfp518b	35.94	ENSMUSG00000094504	Gm5294	0.1
ENSMUSG00000022018	Rgcc	41.02	ENSMUSG00000031737	Irx5	15.81	ENSMUSG00000046668	Cxxc5	59.84	ENSMUSG00000094870	Zfp131	23.96
ENSMUSG00000022053	Ebf2	34.24	ENSMUSG00000031738	Irx6	1.81	ENSMUSG00000046714	Foxc2	12.24	ENSMUSG00000094942	Gm3604	3.37
ENSMUSG00000022061	Nkx3-1	0.45	ENSMUSG00000031832	Taf1c	12.09	ENSMUSG00000046873	Mbtps2	20.59	ENSMUSG00000095139	Pou3f2	24.81
ENSMUSG00000022096	Hr	0.55	ENSMUSG00000031860	Pbx4	24.62	ENSMUSG00000047036	Zfp445	42.88	ENSMUSG00000096014	Sox1	1.49
ENSMUSG00000022228	Zscan26	12.29	ENSMUSG00000031870	Pgr	0.13	ENSMUSG00000047143	Dmrta2	0.1	ENSMUSG00000096225	Lhx8	0.21
ENSMUSG00000022286	Grhl2	0.89	ENSMUSG00000031902	Nfatc3	2.37	ENSMUSG00000047171	Helt	0.12	ENSMUSG00000096433	Gm4944	3.04
ENSMUSG00000022297	Fzd6	5.28	ENSMUSG00000031930	Wwp2	42.62	ENSMUSG00000047342	Zfp286	22.31	ENSMUSG00000096795	Zfp433	20.7
ENSMUSG00000022329	Stk3	21.73	ENSMUSG00000031965	Tbx20	0.15	ENSMUSG00000047407	Tgif1	52.54	ENSMUSG00000096916	Zfp850	7.27
ENSMUSG00000022330	Osr2	0.21	ENSMUSG00000031987	Egln1	15.83	ENSMUSG00000047473	Zfp30	7.2	ENSMUSG00000097084	Foxl1	0.88
ENSMUSG00000022335	Zfat	4.09	ENSMUSG00000032033	Barx2	0.24	ENSMUSG00000047591	Mafa	0.23	ENSMUSG00000098022	Zfp82	7.95
ENSMUSG00000022346	Myc	22.66	ENSMUSG00000032035	Ets1	27.25	ENSMUSG00000048047	Zbtb33	7.85	ENSMUSG00000099083	Atf7	11.03
ENSMUSG00000022361	Zhx1	25.59	ENSMUSG00000032119	Hinfp	13.95	ENSMUSG00000048138	Dmrt2	12.02	ENSMUSG00000100235	Zfp708	3.92
ENSMUSG00000022383	Ppara	0.19	ENSMUSG00000032187	Smarca4	138.4	ENSMUSG00000048249	Crebrf	2.47	ENSMUSG00000101174	Hoxd4	8.89
ENSMUSG00000022389	Tef	10.82	ENSMUSG00000032228	Tcf12	165.62	ENSMUSG00000048251	Bcl11b	7.41			

Supplementary references

Jolma, A., Yan, J., Whitington, T., Toivonen, J., Nitta, K.R., Rastas, P., Morgunova, E., Enge, M., Taipale, M., Wei, G., et al. (2013). DNA-binding specificities of human transcription factors. Cell *152*, 327–339.

Karaz, S., Courgeon, M., Lepetit, H., Bruno, E., Pannone, R., Tarallo, A., Thouzé, F., Kerner, P., Vervoort, M., Causeret, F., et al. (2016). Neuronal fate specification by the Dbx1 transcription factor is linked to the evolutionary acquisition of a novel functional domain. Evodevo 1–13.

Kinameri, E., Inoue, T., Aruga, J., Imayoshi, I., Kageyama, R., Shimogori, T., and Moore, A.W. (2008). Prdm proto-oncogene transcription factor family expression and interaction with the Notch-Hes pathway in mouse neurogenesis. PLoS One *3*, 1–10.

Lu, S., Wise, T.L., and Ruddle, F.H. (1994). Mouse homeobox gene Dbx: sequence, gene structure and expression pattern during mid-gestation. Mech. Dev. *47*, 187–195.

Oosterveen, T., Kurdija, S., Alekseenko, Z., Uhde, C.W., Bergsland, M., Sandberg, M., Andersson, E., Dias, J.M., Muhr, J., and Ericson, J. (2012). Mechanistic differences in the transcriptional interpretation of local and long-range Shh morphogen signaling. Dev. Cell *23*, 1006–1019.

Pierani, A., Brenner-Morton, S., Chiang, C., and Jessell, T.M. (1999). A Sonic Hedgehog–Independent, Retinoid-Activated Pathway of Neurogenesis in the Ventral Spinal Cord. Cell *97*, 903–915.

Pierani, A., Sunshine, M.J., Littman, D.R., Goulding, M., and Jessell, T.M. (2001). Control of Interneuron Fate in the Developing Spinal Cord by the Progenitor Homeodomain Protein Dbx1. *29*, 367–384.

Relaix, F., Polimeni, M., Rocancourt, D., Ponzetto, C., Schafer, B.W., Buckingham, M., and Schäfer, B.W. (2003). The transcriptional activator PAX3-FKHR rescues the defects of Pax3 mutant mice but induces a myogenic gain-of-function phenotype with ligand-independent activation of Met signaling in vivo. Genes Dev *17*, 2950–2965.

Soleimani, V.D., Punch, V.G., Kawabe, Y.I., Jones, A.E., Palidwor, G. a., Porter, C.J., Cross, J.W., Carvajal, J.J., Kockx, C.E.M., van IJcken, W.F.J., et al. (2012). Transcriptional Dominance of Pax7 in Adult Myogenesis Is Due to High-Affinity Recognition of Homeodomain Motifs-supp. Dev. Cell *22*, 1208–1220.

Supplementary Figure Legends

Supp. Fig. 1: Characterisation of AP2α expression profiles in the embryonic dorsal spinal cord and roles of Dbx1 in restricting the generation of dorsal interneurons

A. Immunostaining for AP2α/Sox9/GFP on thoracic sections of GD11.5 Pax3$^{GFP/+}$ embryos showing that Ap2α is induced in the post-mitotic dorsal GFP^{+}, Sox9^{-} neurons of the spinal cord. **B.** Immunostaining for AP2α/Lbx1/Brn3a on brachial sections of GD11.5 wild-type embryos showing that Ap2α expression largely overlaps with the profile of Brn3a and Lbx1 with two exceptions. First, it is excluded from the most ventral Lbx1^{+} cells and its ventral boundary matches that of Brn3a (arrowheads). Hence its ventral expression includes the Brn3a^{+} dI5 IN and excludes the Lbx1^{+}/Brn3a^{-} dI6 IN. Second, it is excluded from the most dorsal cells expressing Brn3a, likely the dI1 IN (arrows). **C.** Immunostaining for AP2α/Lhx2 on brachial sections of GD10.5 wild-type embryos confirming the exclusion of Ap2α from dI1 IN. **D.** Representation of the spinal cord showing the distribution of Ap2α protein in red, characterised by the markers whose D-V extent are depicted in grey. **E.** Immunostaining for Pax2 and FoxD3, as well as GFP detection, on brachial sections of GD11.5 of *Pax3*$^{KIGFP/+}$ and *Pax3*$^{KIGFP/GFP}$;*Pax3*$^{KILacZ/LacZ}$ (dKO) embryos, showing that, in absence of both Pax3 and Pax7 Pax2^{+};GFP^{+} cells express the V1 marker, FoxD3. The white dashed line in **i**, **i'** marks the border between dI5 and dI6 cells; the light green one in **i-ii'** segregates dorsal GFP^{+} cells from the ventral GFP^{-} cells. **F. i-ii** Immunostaining for AP2α/Lbx1/βGalactosidase on brachial sections of GD11.5 *Dbx1*$^{KILacZ/+}$ and *Dbx1*$^{KILacZ/LacZ}$ embryos showing that, in absence of *Dbx1,* p0 progenitors give rise to Lbx1^{+}; AP2a^{-}; Pax2^{+} dI6 interneurons (see brackets in **ii, ii'**). **iii** Quantification of Lbx1^{+}; AP2a^{-} dI6 cells that derive from progenitors that have or have not expressed the βGalactosidase under the control of the *Dbx1* locus (mean±s.e.m., n=4 *Dbx1*$^{KILacZ/+}$ embryos, n=2 *Dbx1*$^{KILacZ/LacZ}$ embryos). **iv.** Immunostaining for Pax2/Lbx1/βGalactosidase on brachial sections of GD11.5 *Dbx1*$^{KILacZ/LacZ}$ embryos showing that Lbx1^{+} neurons derived from p0 progenitors express another dI6 marker, Pax2.

Supp. Fig. 2: Characterisation of Dbx1 profiles in wild-type and Pax3/Pax7 mutant embryos

A. Immunostaining for Dbx1 and Pax7 in thoracic transverse sections of wild-type embryos at the indicated stages. **B-C.** *In situ* hybridisation for *Dbx1* **(B)** and immunolabelling of Dbx1 **(C)** in brachial transverse sections of GD11.5 mouse embryos of the indicated genotype. **D.** Graphs displaying the absolute D-V position from the floor plate in µm of Dbx1 protein

expression in GD11.5 mouse embryos with the indicated genotype (mean ± s.e.m). Scale bars: 50 µm.

Supp. Fig. 3: Pax Position Weight Matrices and response of Dbx1 CRMs to Pax3 and PAX3A

A. Position Weight Matrices retrieved from data generated by Jolma et al. (2013) (1), identified by MEME from ChIP-Seq data generated by Soleimani et al. (2012) (2), or created using MEME by compiling sites previously identified by Soleimani et al. (2012), Moore et al. (2013) and Relaix et al. (2003) (3). **B.** Immunostaining for β-Galactosidase and GFP combined with DAPI labelling performed on sections of chick embryos 24hpe with the indicated reporter constructs carrying *Dbx1* CRMs and either Pax3-GFP **(i-v')** or PAX3A-GFP **(vi-x')**. Scale bars: 50 µm.

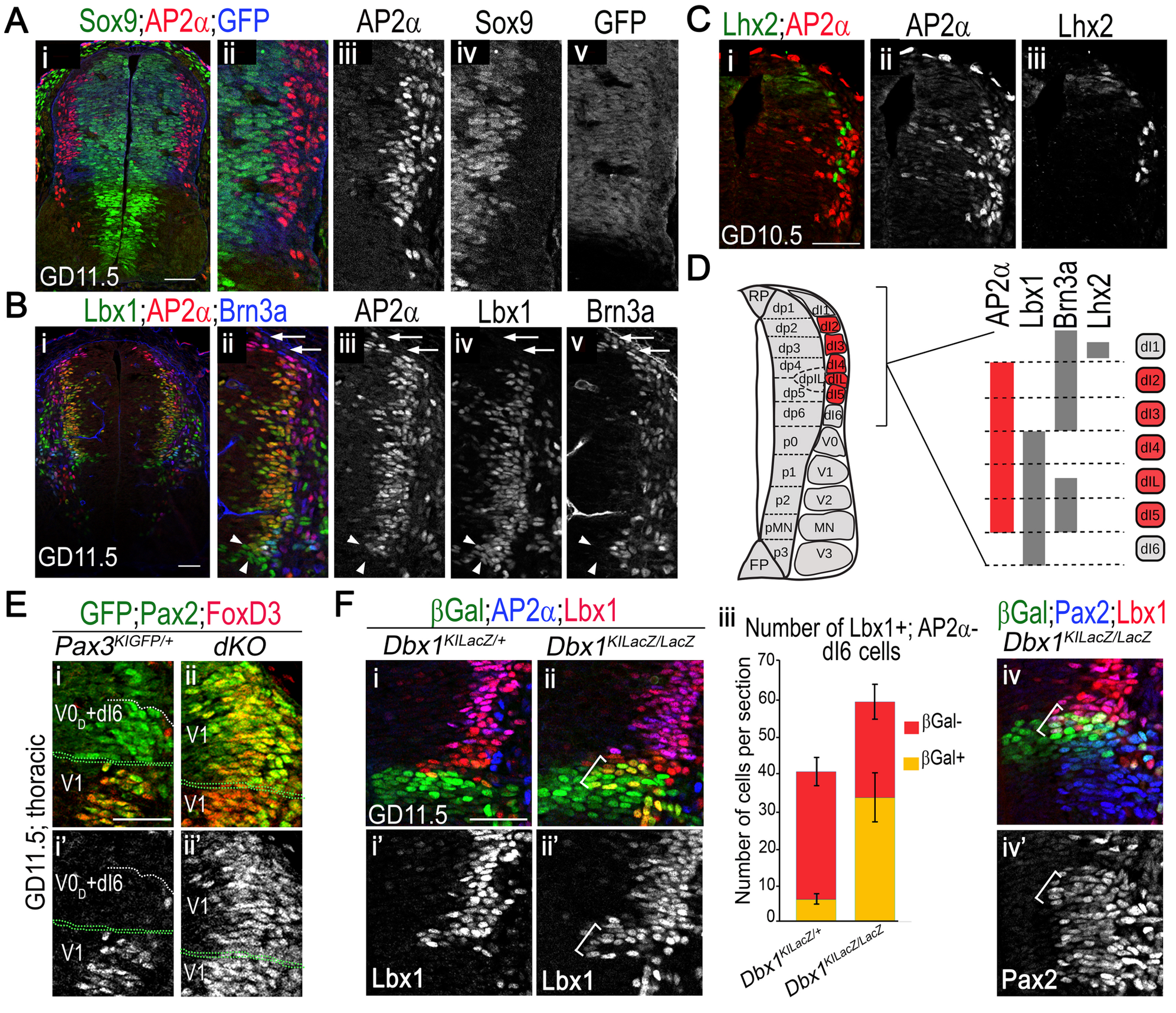

Gard et al., Supp. Figure 1

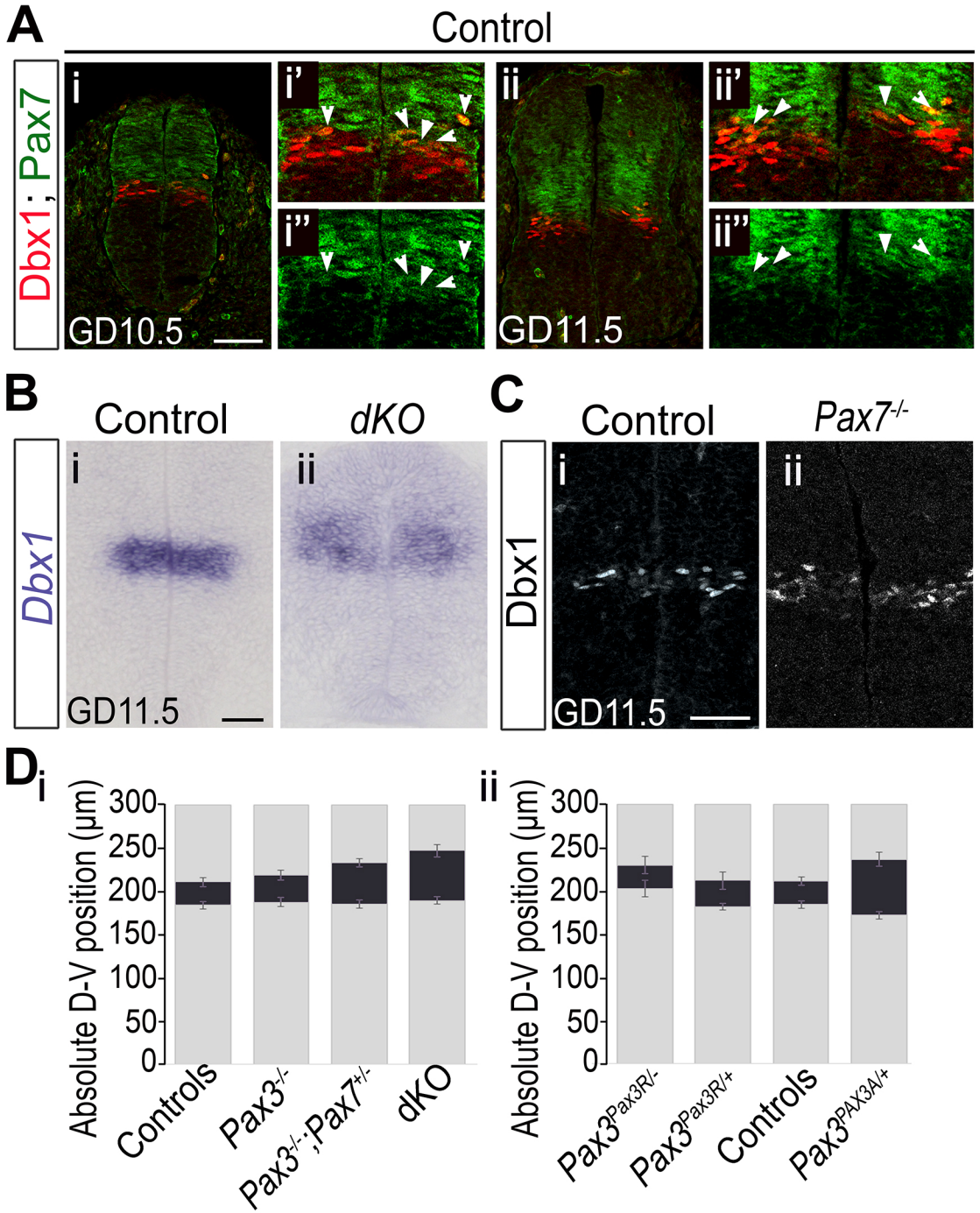

Gard et al., Supp. Figure 2

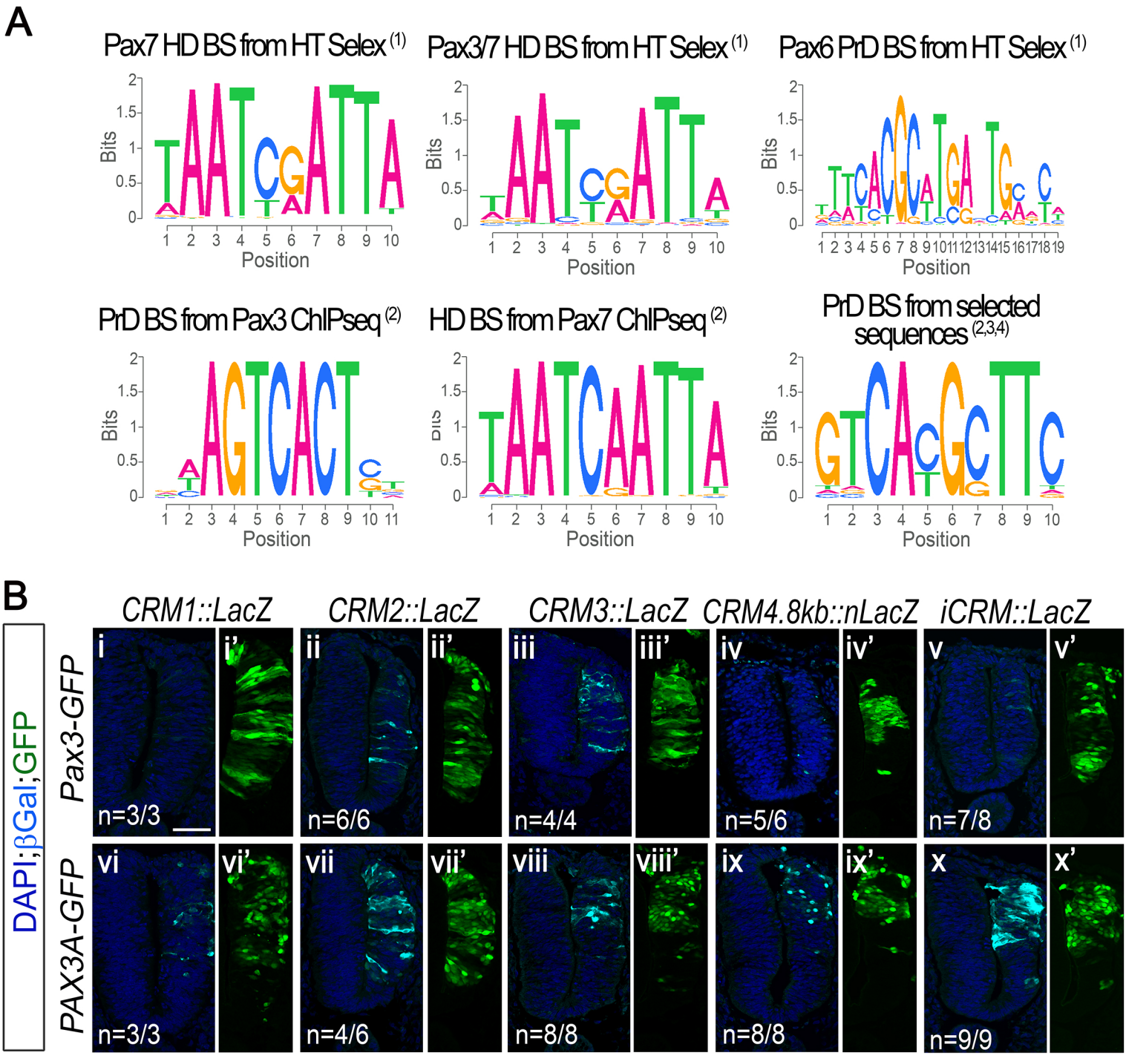

Gard et al., Supp. Figure 3